catalysts

MDPI

Review

Recent Progress in the Steam Reforming of Bio-Oil for Hydrogen Production: A Review of Operating Parameters, Catalytic Systems and Technological Innovations

Anastasia Pafili [1], Nikolaos D. Charisiou [1,*], Savvas L. Douvartzides [1,2], Georgios I. Siakavelas [1,3], Wen Wang [4], Guanqing Liu [4], Vagelis G. Papadakis [3] and Maria A. Goula [1,*]

1 Laboratory of Alternative Fuels and Environmental Catalysis (LAFEC), Department of Chemical Engineering, University of Western Macedonia, GR-50100 Kozani, Greece; aepafili@gmail.com (A.P.); sdouvartzidis@uowm.gr (S.L.D.); giorgosiakavelas@gmail.com (G.I.S.)
2 Department of Mechanical Engineering, University of Western Macedonia, GR-50100 Kozani, Greece
3 Department of Environmental Engineering, University of Patras, GR-30100 Agrinio, Greece; vgpapadakis@upatras.gr
4 Biomass Energy and Environmental Engineering Research Center, Beijing University of Chemical Technology, Beijing 100029, China; wangwen@buct.edu.cn (W.W.); gqliu@mail.buct.edu.cn (G.L.)
* Correspondence: ncharisiou@uowm.gr (N.D.C.); mgoula@uowm.gr (M.A.G.)

Abstract: The present review focuses on the production of renewable hydrogen through the catalytic steam reforming of bio-oil, the liquid product of the fast pyrolysis of biomass. Although in theory the process is capable of producing high yields of hydrogen, in practice, certain technological issues require radical improvements before its commercialization. Herein, we illustrate the fundamental knowledge behind the technology of the steam reforming of bio-oil and critically discuss the major factors influencing the reforming process such as the feedstock composition, the reactor design, the reaction temperature and pressure, the steam to carbon ratio and the hour space velocity. We also emphasize the latest research for the best suited reforming catalysts among the specific groups of noble metal, transition metal, bimetallic and perovskite type catalysts. The effect of the catalyst preparation method and the technological obstacle of catalytic deactivation due to coke deposition, metal sintering, metal oxidation and sulfur poisoning are addressed. Finally, various novel modified steam reforming techniques which are under development are discussed, such as the in-line two-stage pyrolysis and steam reforming, the sorption enhanced steam reforming (SESR) and the chemical looping steam reforming (CLSR). Moreover, we argue that while the majority of research studies examine hydrogen generation using different model compounds, much work must be done to optimally treat the raw or aqueous bio-oil mixtures for efficient practical use. Moreover, further research is also required on the reaction mechanisms and kinetics of the process, as these have not yet been fully understood.

Keywords: renewable hydrogen; bio-oil steam reforming; steam reforming catalysts; two-stage in-line pyrolysis and reforming; sorption enhanced steam reforming; chemical looping steam reforming

check for updates

Citation: Pafili, A.; Charisiou, N.D.; Douvartzides, S.L.; Siakavelas, G.I.; Wang, W.; Liu, G.; Papadakis, V.G.; Goula, M.A. Recent Progress in the Steam Reforming of Bio-Oil for Hydrogen Production: A Review of Operating Parameters, Catalytic Systems and Technological Innovations. *Catalysts* **2021**, *11*, 1526. https://doi.org/10.3390/catal11121526

Academic Editor: Ken-ichi Fujita

Received: 22 November 2021
Accepted: 11 December 2021
Published: 15 December 2021

Publisher's Note: MDPI stays neutral with regard to jurisdictional claims in published maps and institutional affiliations.

Copyright: © 2021 by the authors. Licensee MDPI, Basel, Switzerland. This article is an open access article distributed under the terms and conditions of the Creative Commons Attribution (CC BY) license (https://creativecommons.org/licenses/by/4.0/).

1. Introduction

The decarbonization of our global energy market and the exploitation of renewable energy sources (RES) are widely considered as the most important policies which can bring our planet into a secure sustainable future [1–3]. Renewable energy, such as solar, wind, tidal and geothermal, will inevitably play a decisive role in the next decades, but clean and effective technologies are also necessary for the supply of alternative transportation biofuels [4–7].

Lignocellulosic biomass, such as agricultural residues and dedicated energy crops, has a vast unused potential for continuous energy supply at a low price and with neutral

carbon dioxide (CO_2) environmental impact [8–10]. The utilization of lignocelluloses can open a renewable carbon-neutral roadmap [11,12] for the production of heat, electrical power and biofuels. The conversion of biomass to renewable hydrogen (H_2) is of major interest as it can be used as a fuel in combustion engines and fuel cells or may be used for the synthesis of useful chemicals and high energy density transportation biofuels [13,14]. Hydrogen is the cleanest fuel available since its utilization produces only steam vapors and does not pollute the atmosphere with CO_2, greenhouse gases or other emissions [15–21].

An empirical chemical formula of biomass can be written as $C_nH_mO_k \cdot xH_2O$ [22,23] and typical biomass compositions are given in Table 1. Depending on the characteristics of the raw feedstock, lignocellulosic biomass can be treated for the production of high value biofuels and bio-chemicals using several thermochemical or biochemical processes.

Table 1. Composition of woody, herbaceous and waste biomass. Adopted from ref. [24].

Feedstock Composition	Woody	Herbaceous	Wastes
	Proximate		
Volatiles (%)	84.0	79.1	76.7
Ash (%)	1.3	5.5	6.6
Fixed carbon (%)	14.7	15.4	14.8
	Ultimate		
H (%)	6.0	5.8	5.9
C (%)	50.7	47.4	46.0
N (%)	0.32	0.75	1.3
O (%)	41.9	41.0	38.3
S (%)	0.03	0.10	0.15
	Structural		
Cellulose (%)	51.2	32.1	28.4
Hemicellulose (%)	21.0	18.6	16.4
Lignin (%)	26.1	16.3	12.5

Conversion technologies that rely on thermochemical methods, such as gasification and pyrolysis, are able to convert the entire lignocellulosic matter into gaseous and liquid products, which can be used directly as transport fuels or may serve the synthesis of upgraded biofuels [25–29]. Conventional and catalytic fast pyrolysis technologies especially, lead to the formation of a condensed liquid product known as bio-oil (tar or pyrolytic oil), which serves as an intermediate for the generation of hydrogen and upgraded transportation biofuels.

The present article reviews the recent trends and research outputs in the technology of hydrogen production through the catalytic steam reforming (SR) of bio-oil. The review discusses the most important steam reforming processing parameters such as the reactor feed composition, the reactor design and the reaction conditions and presents the recent research findings on the development of effective catalysts. Information on noble, transition, bimetallic and perovskite type catalysts is critically presented, and specific attention is paid to the effect of the catalyst preparation method and the recent progresses against catalyst deactivation through coke formation, metal sintering, metal oxidation and sulfur poisoning. The critical examination of the available literature reveals that while in theory the process is capable of producing high yields of hydrogen, in practice certain technological issues require further investigation and radical improvements before its commercialization. A major challenge is the high chemical complexity of raw bio-oil, which does not readily allow a systematic approach on the maximization of hydrogen productivity and the alleviation of carbon deposition issues. Moreover, raw bio-oil cannot be completely vaporized and when heated leads to the formation of residual solids which accelerate catalyst poisoning at rates much higher than the usually examined model compounds. Additional research is also required on the reaction mechanisms and kinetics, which have not yet been fully

understood and much work must be done to optimally treat the raw or aqueous bio-oil mixtures for efficient practical use. Finally, further consideration must be given to identify catalysts with low cost, high activity and stability, strong regenerative ability and extensive operating lifetime for successful operation in industrial conditions. Since catalyst deactivation is a major problem encountered during the steam reforming process, the mechanisms of coke formation and metal sintering should also be further investigated. However, the challenges outlined herein must be met with increased vigor as the efficient production of renewable hydrogen promises to help move away from the current, fossil-based model of energy production.

2. Bio-Oil Properties and Composition

Biomass can be converted into hydrogen via two major thermochemical routes: (i) gasification, to directly produce syngas, and (ii) pyrolysis, to obtain bio-oil, followed by reforming. An excellent review of the major biomass to hydrogen production processes has been provided by Martino et al. [30]. Biomass pyrolysis takes place between 220 and 900 °C, in the absence of O_2. During the process, hemicellulose, cellulose, and lignin biopolymers thermally decompose to form a solid residue (charcoal or biochar), condensable gases and non-condensable/permanent gases (e.g., CO_2, CO, H_2 and other light hydrocarbons). After cooling at room temperature, the non-permanent gases are condensed to form the bio-oil, a liquid phase product of higher energy density than biomass [25,31]. Bio-oil is a dark brown liquid of high viscosity, comprised of a plethora of heavy organic and inorganic molecules and, hence, it is a suitable platform source for many upgraded chemicals. The composition of bio-oil and its properties depend on the raw feedstock composition and the conditions at which pyrolysis was undertaken, such as temperature, heating rate, and residence time [32]. Compounds in bio-oil include carboxylic acids, aldehydes, alcohols, ketones, anhydrosugars and substituted furans derived from cellulose and hemicellulose, and phenolics and cyclic oxygenates derived from lignin. The most abundant species are acetic acid, acetone, acetol, glycolaldehyde, furanones, levoglucosan, and phenol [33–37].

Water addition can help separate the bio-oil into two distinct fractions. The first fraction is the hydrophilic carbohydrate or aqueous phase containing typically 20 wt.% organics, which can be catalytically steam reformed. The second fraction, often called pyrolytic lignin is the hydrophobic organic phase and contains furan and aromatic based species; this fraction can be used for the development of a plethora of products [38,39]. As raw bio-oil cannot be totally vaporized, the solids that remain as residuals can cause clogging in the feeding lines and the reactor. In addition, despite the higher H_2 yields obtained from the reforming of the whole oil, the SR of the bio-oil aqueous fraction is preferred in several studies [40–47]. Table 2 summarizes the characteristics of both the raw bio-oil and its aqueous fraction, while Table 3 provides a typical composition of raw bio-oil.

Table 2. Raw bio-oil characteristics [48].

Parameter	Bio-Oil	Aqueous Fraction of Bio-Oil
pH	2.6	2.5
Water content (wt. %)	36	84
	Ultimate analysis (wt. %)	
Carbon	36.07	7.35
Hydrogen	8.45	10.82
Nitrogen	0.11	0.00
Oxygen [1]	55.37	81.83

[1] Determined by difference.

Generally, bio-oil consists of organic components rich in oxygen (30–40 wt. %), tars (e.g., naphthalene, toluene and benzene), and water (approximately 25 wt. %). The presence of organic acids decreases the bio-oil pH at 2.5–3.0 and causes corrosion and storage issues. Compared with the fossil petroleum distillates, crude bio-oil has a very large oxygen content and its heating value is only around 16 MJ/kg, i.e., almost 2.7 times lower than that

of typical fossil diesel fuel [31,50]. Therefore, before final use the stability and combustion properties of bio-oil need to be enhanced; this is achieved by reducing its water and oxygen content. Kumar and Strezov [51] and Lian et al. [52] provide information on the methods currently employed for the upgrading of bio-oil regarding the production of valorized fuels. Catalytic fast pyrolysis is regarded as the most encouraging method for the efficient production of bio-oil (Figure 1). The atmosphere in which the reaction takes place needs to be inert, while the temperatures can be between 400 and 600 °C. High heating and cooling rates (1000–10,000 K/s) and short residence times (1–2 s) are also necessary. This process helps obtain liquid with a yield of up to about 75 wt.%; the yield for the gas and for the char products is typically between 10 and 20 wt. % and 10 and 15 wt. %, respectively [53]. In recent years, the coupling of the fast pyrolysis of biomass with the catalytic SR of the pyrolytic oils has received considerable attention [26,31,54].

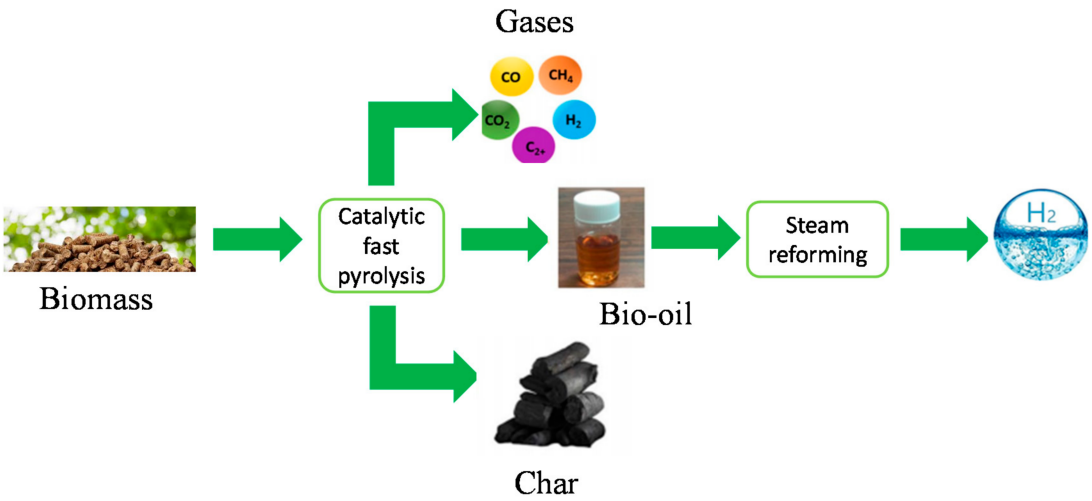

Figure 1. Schematic representation of the fast pyrolysis of biomass for H_2 production.

Due to the complexity of bio-oil, previous studies usually focus on the use of model compounds. The most studied of these compounds is acetic acid as it is one of the main constituents of bio-oil [39,55–82]. Numerous literature reports can also be found concerning the steam reforming of bio-alcohols such as methanol [14,56,58,72], ethanol [14,58,70,83–88] and glycerol [14,89–94]. The reforming of acetone has also attracted considerable attention [56,58,63,69,70,77,95–97]. Other model compounds systematically tested include hydroxyacetaldehyde, cellulose and lignin [72], phenol [70,74,98], acetol [38,74,99], m-cresol, furfural and guaiacol [58,89]. The use of model compounds, i.e., knowing exactly the composition of the feed entering the reactor, also provides the advantage that it allows the comparison of different catalytic systems, provided that similar experimental conditions are used. The analysis of the liquid products is also less complex as the number of products is limited [23,53].

3. Mechanism of Bio-Oil Steam Reforming

A major advantage of the production of hydrogen through catalytic SR is that bio-oil dehydration, a rather expensive process, can be avoided [100]. Steam reforming (SR) is an endothermic equilibrium reaction between an organic compound and steam in the presence of a catalyst. It results in the formation of a mixture of hydrogen and carbon monoxide (Equation (1)) and, usually, it is accompanied by the water gas shift reaction (Equation (2)) [101,102]:

$$C_nH_mO_k + (n - k)\,H_2O \rightarrow nCO + (n + m/2 - k)\,H_2 \quad (1)$$

$$nCO + nH_2O \leftrightarrow nCO_2 + nH_2 \quad (2)$$

The general chemical reaction for the steam reforming of bio-oil is as follows [15,95]:

$$C_nH_mO_k + (2n - k)\ H_2O \rightarrow nCO_2 + (2n + m/2 - k)\ H_2 \quad (3)$$

Generally, other undesirable reactions take place when oxygenates react over a metal surface and so the hydrogen yield is lower than the stoichiometric yield. Carbon monoxide and dioxide methanation (Equations (4) and (5)), methane reforming (Equations (6) and (7)), and C_2 steam reforming (Equation (8)) are amongst the secondary reactions that occur during bio-oil steam reforming [44]. A major issue is carbon deposition, which can lower hydrogen production and shorten the catalyst life expectancy. The partial thermal decomposition of oxygenates (Equation (9)) and the Boudouard reaction (Equation (10)) are the main solid carbon forming reactions [53].

$$CO + 3H_2 \rightarrow CH_4 + H_2O \quad (4)$$

$$CO_2 + 4H_2 \rightarrow CH_4 + 2H_2O \quad (5)$$

$$CH_4 + 2H_2O \rightarrow CO_2 + 4H_2 \quad (6)$$

$$CH_4 + CO_2 \rightarrow 2CO + 2H_2 \quad (7)$$

$$C_2H_n + 2H_2O \rightarrow 2CO + (n/2 + 2)\ H_2 \quad (8)$$

$$C_nH_mO_k \rightarrow C_xH_yO_z + \text{gases}\ (H_2, CO, CO_2, CH_4) + \text{coke} \quad (9)$$

$$2CO \rightarrow C + CO_2 \quad (10)$$

Carbon deposits are also produced from methane decomposition (Equation (11)), carbon monoxide and dioxide decomposition (Equations (12) and (13)), and ethene polymerization (Equation (14)) [12].

$$CH_4 \leftrightarrow C + 2H_2 \quad (11)$$

$$CO + H_2 \leftrightarrow C + H_2O \quad (12)$$

$$CO_2 + 2H_2 \leftrightarrow C + 2H_2O \quad (13)$$

$$nC_2H_4 \rightarrow \text{Carbon} \quad (14)$$

Bio-oil oxygenates conversion is given as the ratio of the moles of carbon converted to products (gaseous and liquids) to the moles of carbon in the feed, as shown in Equation (15). Alternatively, conversion can be calculated by the quantity of organic feed that remains unconverted in the liquid effluents [63]. Catalytic activity may also be gauged by the calculation of H_2 selectivity, which is the percentage molar or mass concentration of hydrogen in the product stream. The selectivity (Equation (16)) of a product is in relation to the other competing products, while the yield (Equation (17)) calculation is based on the quantity of feed [23].

$$\%\ \text{Conversion} = \frac{\text{moles of carbon in the product gas}}{\text{moles of carbon in the feed}} \times 100\ \% \quad (15)$$

$$\%\ \text{X Selectivity} = \frac{\text{amount of X}}{\text{total amount of syngas (dry} - \text{basis)}} \times 100\ \% \quad (16)$$

$$\%\ \text{X Yield} = \frac{\text{amount of X produced}}{\text{theoritical amount of X produced}} \times 100\ \% \quad (17)$$

In Equations (16) and (17) X represents the products found at the outlet of the reactor (e.g., H_2, CO, CO_2, CH_4). The yield of hydrogen cannot be equal to the stoichiometric maximum because of the undesirable production of CO and CH_4 which are formed during reforming via reverse water gas shift and methanation reactions [63].

4. Operating Parameters Affecting Bio-Oil Steam Reforming

The operating parameters affecting the SR of bio-oil include the composition of the feedstock, the reactor type, the reaction temperature, the space velocity and the steam to carbon (S/C) ratio, which means that in the effort to approach stoichiometric yields, a wide range of combinations have been tested. Generally, a higher bio-oil conversion is favored at higher reforming temperatures, low pressures and higher steam to carbon ratios.

4.1. Effect of the Feed Composition

Comparative studies on the SR of different organic molecules derived from bio-oil (e.g., furfural, formic acid, methanol, acetic acid, ethanol, acetaldehyde, guaiacol, acetone) have demonstrated that the molecular structures have a large influence on the reactivity and tendency to coking. Bimbela et al. [38,39] investigated acetic acid, acetol and n-butanol steam reforming using co-precipitated Ni/Al_2O_3 catalysts of different Ni contents (23, 28 and 33%) and concluded that reactivity followed the order: acetic acid > acetol > n-butanol (Figure 2); the rate of catalyst deactivation due to coke deposition followed the opposite trend. Similarly, Baviskar and Vaidya [103] reported that the conversion of oxygenates with different functional groups was butyraldehyde > ethyl acetate > 1-methoxy-2-propanol > 2-butanone; coke formation followed the opposite trend. These results suggest that carbonyls are easier to convert in comparison with hydroxyls.

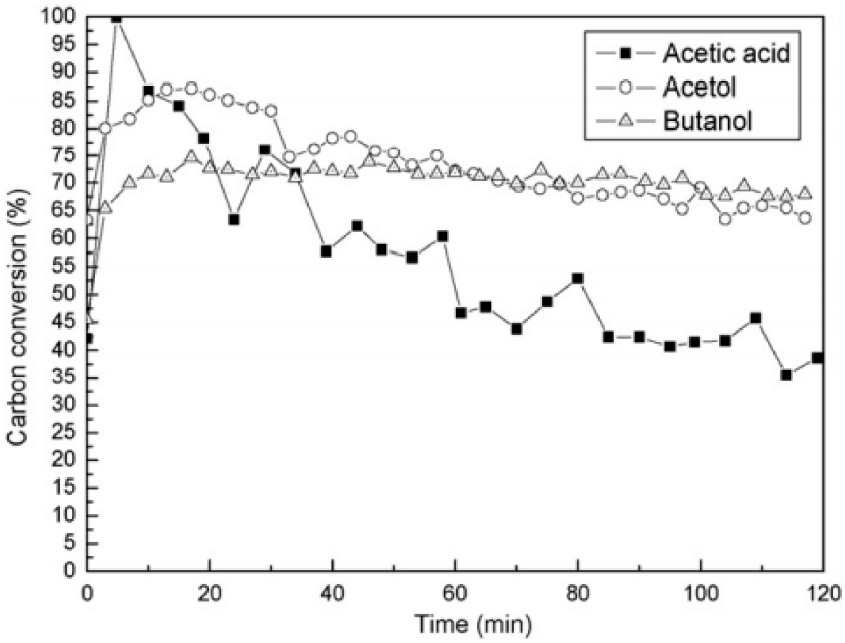

Figure 2. Comparison of the dependence of carbon conversion with time for acetic acid, acetol and n-butanol tested at GHSV around 30,000 h^{-1}, 650 °C and 33%Ni/Al_2O_3 catalyst. Reproduced with permission from [38]. Copyright Elsevier, 2021.

The effect that molecular structures have on the conversion of formic, acetic, propionic and butyric acids (i.e., carboxylic acids) during steam reforming, was examined by Li et al. [55]. It is noted that carboxylic acids are usually found at around 5 wt. % in bio-oil, which means that the clarification of their reaction behavior is essential for the optimization of the SR process. The authors concluded that an increase in the length of the aliphatic chain led to a decrease in the conversion rate (Figure 3).

Zhang et al. [58] carried out a study on the steam reforming of methanol, formic acid, acetone, acetic acid, acetaldehyde, ethanol, furfural and guaiacol and concluded that the structure of the feed molecules has a significant impact on reactivity, with methanol and formic acid reformed at low temperatures due to the absence of the cracking of C-C bonds involved in their conversion. Li et al. [56] supported the above finding as they concluded

that the reforming of acetic acid is relatively easier in comparison to that of acetone, as the former has a lower molecular size. Ortiz-Toral et al. [40] also observed that aqueous bio-oil fractions with higher concentrations of lower molecular-weight oxygenates, such as acetic acid and acetol, converted more effectively into H_2, whereas the existence of heavier molecules, such as levoglucosan, furfural and phenolics compounds significantly impacted the time-on-stream catalytic stability. Moreover, the large oxygenate compounds contained in bio-oil do not vaporize easily upon entering the reactor, which means that there is a risk of blockage in the feeding line and/or the reactor by residual solids [72]. Table 4 summarizes the effect of different model compounds as feedstock in the steam reforming process.

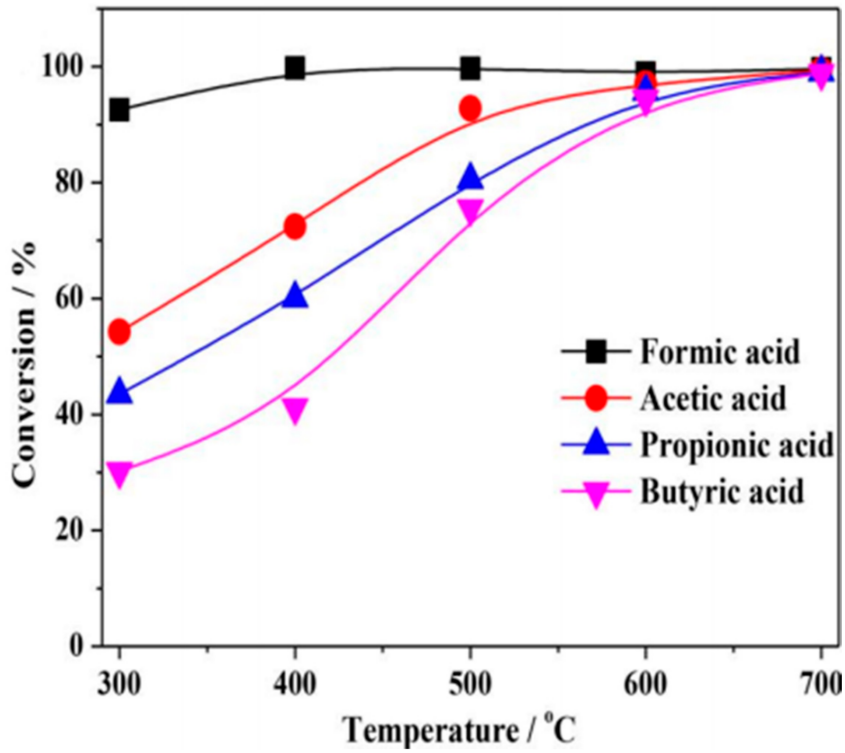

Figure 3. Comparison of the dependence of carbon conversion with temperature for four carboxylic acids tested at S/C = 5, LHSV = 12.7 h^{-1}, P = 1 atm and 20% Ni/Al_2O_3 catalyst. Reproduced with permission from [48]. Copyright Elsevier, 2021.

Table 3. Raw bio-oil composition, as derived from the fast pyrolysis of pine wood. Adopted from [12,22,23,25,49].

Components	wt. %
Acetic acid	15.0–15.5
Acetone	5.0–5.5
Alcohols	12.0–12.5
Ethers	0.5–1.0
Hydroxyacetaldehyde	10.5–11.0
Levoglucosane	3.5–4.0
Other acids and esters	10.5–11.0
Other aldehydes	9.5–10.0
Other ketones	21.5–22.0
Others	1.0–1.5
Phenols	6.5–7.0
Unidentified	1.0–1.5

Table 4. Summary of the literature on the effect of different model compounds as feedstocks in the steam reforming process.

Type of Feed [1]	Catalyst [2]	Experimental Conditions	Comments	Ref.
acetic acid, acetol and n-butanol, separately	23, 28 and 33% Ni/Al_2O_3	fixed bed quartz reactor; 0–8.70 g catalyst min/g model compound; feeding rate: 0.15, 0.17, 0.23 mL/min; GHSV = 28,500, 20,000, 57,000 h^{-1}; S/C = 5.58, 14.70; P = 1 atm; T = 550–750 °C	28% Ni provide the highest H_2 yield at 650 °C. Increasing temperature enhanced the yields to H_2, CO and CO_2.	[38,39]
2-butanone, 1-methoxy-2-propanol, ethyl acetate, butyraldehyde, separately	20% Ni/Al_2O_3	fixed bed quartz reactor; 1.5 g of catalyst; flow rate: 0.25–1 mL/min; S/C = 15–25; P = 1 atm; T = 350–500 °C	45.4% H_2 yield at 500 °C with 2-butanone; 51.1% H_2 yield at 500 °C with 1-methoxy-2-propanol; 52.8% H_2 yield at 500 °C with ethyl acetate; 54.2% H_2 yield at 500 °C with butyraldehyde	[103]
formic acid, acetic acid, propionic acid and butyric acid, separately	20% Ni/Al_2O_3	fixed bed quartz reactor; 500 mg of catalyst LHSV = 12.7 h^{-1}; GHSV = 49,317 h^{-1} at 300 °C and 79,848 h^{-1} at 700 °C; S/C = 5; P = 1 atm	The increase of the length of the aliphatic carbon chain inhibited reforming reactions, led to lower yields of H_2 and to increased coking.	[55]
methanol, ethanol, formic acid, acetic acid, acetaldehyde, acetone, furfural, guaiacol, separately	15% Ni-5% La/Al_2O_3	fixed bed quartz reactor; 0.5 g of catalyst; flow rate: 0.12 mL/min; LHSV = 12.7 h^{-1}, S/C = 5; P = 1 atm; T = 300–600 °C	The reforming of methanol and formic acid was achieved at a low temperature; coking was minimized. Ethanol, acetic acid, acetaldehyde or acetone required higher reforming temperatures; significant coke deposition, especially for acetone or acetaldehyde. The coke derived during the SR of furfural and guaiacol was more graphite-like (difficult to oxidize)	[58]
methanol, acetic acid, acetone separately	15% Mn/Al_2O_3, 15% Fe/Al_2O_3, 15% Co/Al_2O_3, 15% Ni/Al_2O_3, 15% Cu/Al_2O_3, 15% Zn/Al_2O_3 and unsupported Mn, Fe, Co, Ni, Cu, Zn	fixed bed quartz reactor; 0.50 g of catalyst; flow rate: 0.12 mL/min; LHSV = 12.7 h^{-1}; S/C = 5; P = 1 atm	Ni and Co catalysts were more active than Mn, Fe or Zn. Alumina helped enhance metal dispersion. Coke formed during the SR of acetic acid was more aromatic than that formed during the SR of acetone.	[56]
bio-oil aqueous fraction	11% Ni/Al_2O_3	fixed bed quartz reactor; WHSV = 0.87 h^{-1}; flow rate: 4.0 mL/h; S/C = 4, 8, 12,18; T = 500–700 °C	H_2 production was enhanced when low MW species (acetic acid and acetol) were used and declined when higher MW species (levoglucosan and furfural) were used.	[40]

[1] aqueous solution of every model compound is used as feedstock; [2] wt. %.

4.2. Effect of the Reactor Type

As mentioned above, coke deposition is a major obstacle in the SR of bio-oil or its model compounds as it leads to the deactivation of the catalyst and the fouling of the reactor. To avoid reactor fouling, a variety of specially designed reactors have been proposed. These include two-stage pyrolysis-reforming, separate fixed bed and fluidized bed reactors, micro-reactors, and membrane, spouted bed, and nozzle-fed reactors [23,26,104]. Fixed bed reactors are more commonly used and, as shown in Figure 4, they are typically made up of a cylindrical vessel packed with catalyst pellets. However, fixed bed reactors are susceptible to coke deposition over the catalyst surface, limiting the operating time and hydrogen yield due to the large amount of residue formed, especially when reforming larger model compounds or crude bio-oil [105]. Thus, this type of reactor is preferred for the reforming of lighter model compounds, such as acetic acid and ethanol. In contrast, fluidized bed reactors with continuous operation tackle

the reactor blockage by the gasification of carbonaceous deposits [104,106,107]. Comparing these two types of reactors, fixed bed reactors are easy to design, control, and operate and have lower maintenance costs, but coke formation is a challenging issue.

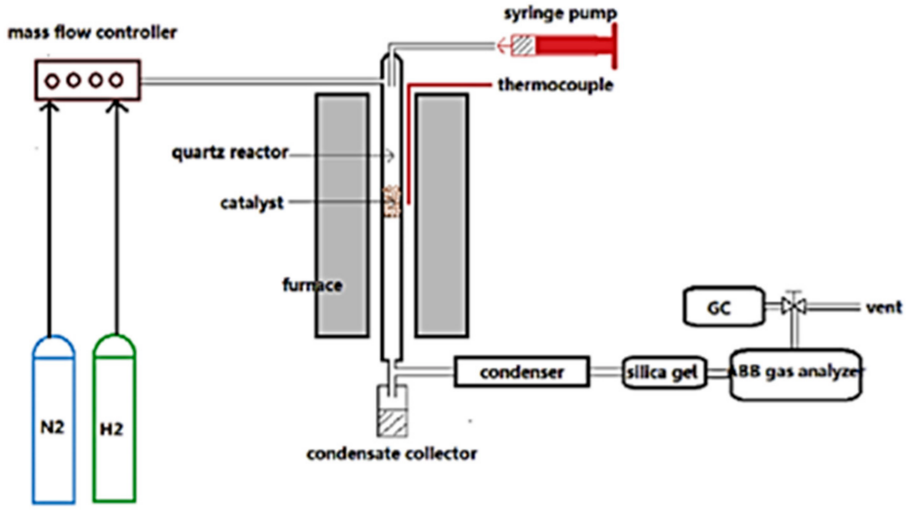

Figure 4. Schematic diagram of a typical fixed-bed reactor. Reproduced with permission from [79]. Copyright Elsevier, 2021.

A triple-nozzle spraying system has also been employed for the aqueous bio-oil fraction [108,109] with Basagiannis et al. [109] arguing that carbon deposition is minimized to a great extent when the liquid is fed into the reactor using high flow rate nozzles. Moreover, Kechagiopoulos et al. [110,111] examined the SR of ethylene glycol and the aqueous phase of bio-oil in a pilot scale spouted bed reactor and argued that surface carbon can be minimized if the hot particles are rapidly mixed with cold reactants along and the constant cyclical movement of solid particles.

4.3. Effect of Temperature

Being an endothermic process, the SR of bio-oil is carried out at high temperatures. Thermodynamics suggest that the yield to hydrogen is maximized around 550 °C, above this temperature, the yield gradually declines due to coke formation and the competing thermal cracking reactions of the organic compounds [78]. Lower temperatures should be avoided as they favor the formation of unstable by-products through decomposition and dehydration of the feed molecules. The presence of high amounts of steam in the process can favor the water-gas shift reaction and the hydrogen produced can combine with CO to generate CH_4. The water-gas shift reaction and methanation are both exothermic reactions and take place at low temperatures. When the reaction temperature is below 500 °C, CH_4 is the thermodynamically favored product. With a rise in temperature, H_2 and CO_2 formations increase [51]. The reactivity of the organic molecules is also affected by their molecular structures. For example, methanol and formic acid require lower temperatures for their reforming, while ethanol, acetic acid, acetaldehyde, or acetone require higher temperatures to crack the C-C bonds in the aliphatic carbon chain [55,58].

4.4. Effect of Pressure

Vagia and Lemonidou [112,113] have conducted thermodynamic studies and investigated the effect of pressure on the steam reforming process. According to the authors, the equilibrium shifts in favor of the lighter chemical species, such as hydrogen, when the pressure is lowered. Thus, the SR of bio-oil is usually carried out at atmospheric pressure, which enhances H_2 selectivity and ensures the optimum yield. Higher pressures lead to a drop in hydrogen production.

4.5. Effect of Space Time and Liquid Feed Rate

Space time is another important variable that affects the SR of bio-oil. A high space time promotes the reforming and the WGS reactions, and hence improves the hydrogen yield. At low space velocity values, the RWGS reaction is favored, which leads to an increase in CO concentration and a decrease in CO_2. Meanwhile CH_4 and light hydrocarbons (secondary products produced mainly from cracking reactions) disappear [22,54].

The effect of the rate at which liquid is fed has also been investigated. It is known that the partial pressure in the reaction bed is increased when a higher liquid feed rate is used and since the rate of the reaction depends directly on the concentration of reactants, the hydrogen yield is increased [102]. In general, the steam reforming performance will approach the thermodynamic equilibrium if sufficient contact time is allowed between the feedstock and the catalyst.

4.6. Effect of the Steam-to-Carbon Ratio

The steam to carbon (S/C) ratio is a critical process parameter that determines the distribution of products. This is because the feedstock used and the steam contest for the active sites exist on the surface of the catalyst [12]. The S/C ratio (Equation (18)) is given by dividing the amount of steam by the total amount of carbon in the feedstock (taking into account the H_2O content) [23].

$$\mathrm{S/C} = \frac{\text{amount of steam}}{\text{total amount of carbon in the feed (wet basis)}} \tag{18}$$

The H_2 yield can be maximized by promoting the WGS reaction, which requires the use of high steam partial pressure (high S/C ratio) as it favors the adsorption of steam on the catalyst active sites. On the other hand, the use of low S/C values favors the decomposition of the feedstock, which promotes the formation of CH_4 and CO and diminishes the yield to H_2 [102]. Moreover, low S/C ratios also promote the deposition of carbon. On the contrary, high S/C ratios can promote the gasification of solid carbon [114]. However, the drawback of using a high S/C ratio is that additional energy and heat are required to separate the steam from the products [115,116].

5. Catalyst Developments in the Bio-Oil Steam Reforming

As is well understood, the ideal bio-oil reforming catalyst should exhibit: (i) high reforming activity, (ii) high selectivity towards hydrogen generation, (iii) resilience towards deactivation by carbon deposition and/or metal particle sintering, and (iv) the ability to cope with the presence of O_2-containing functional groups. The following subsections provide an overview of the state of the art and the recent advances made on the utilization and development of bio-oil steam reforming catalysts.

5.1. Noble Metal-Based Catalysts

Noble metals such as Ru, Pt, Pd, Rh and Ir are known to exhibit high catalytic activity and hydrogen selectivity during the SR of bio-oil, as they have exceptional ability to cleave the C-C bonds. Moreover, noble metals show low propensity to form coke [64,68–70,95,109]. Jeong and co-workers [117] proved that the activity during the SR of acetic, propionic and butyric acid, decreased in the order of Ru > Pd ~ Rh > Pt > Ni. Vagia et al. [63] investigated the steam reforming of acetic acid and acetone using catalytic systems with 5 wt. % Ni and 0.5 wt. % Rh that were based on $CaO{\cdot}2Al_2O_3$ and $12CaO{\cdot}7Al_2O_3$. The authors concluded that the Rh-based catalyst was more active at higher temperatures than Ni in the SR of acetic acid but provided only a slightly higher H_2 yield in the SR of acetone. The catalysts that included noble metals as part of the active phase also showed the lowest coke deposition.

The nature of the support also plays a major role in the reforming reactions and basic oxides, such as La_2O_3, CeO_2, MgO and CaO, have generally been shown to enhance the SR activity. Moreover, the addition of alkali species can modify the interaction between the adsorbed species and the active metal. Basagiannis and Verykios [81] compared

the performances of Pd, Pt, Ru, Rh and Ni-based catalytic systems supported on Al_2O_3 modified with La, Mg and Ce in the SR of acetic acid and showed that the most active systems were those based on Ni, Rh and Ru. Moreover, the authors were able to prove that the catalytic systems based on La_2O_3/Al_2O_3 and MgO/Al_2O_3 remained active during long-term stability tests.

Vagia and Lemonidou [64] used CeO_2–ZrO_2-mixed oxides as supporting material and prepared catalytic systems with Ni and Rh as active phase. The authors then tested the performance of these systems in the SR of acetic acid and observed low carbon deposition after stability tests. The authors concluded that this was due to the synergy of the support and metal, which enhanced the oxygen exchange reactions. In another interesting work, Rioche et al. [70] reported the highest H_2 yield (75%) at 800 °C using Rh, Pd and Pt catalysts supported on $CeZrO_2$, which was significantly higher in comparison to Al_2O_3-based catalysts. Takanabe et al. [68,69,95] suggested a bifunctional mechanism for the SR of acetic acid over Pt/ZrO_2 catalysts. Specifically, the authors argued that the activation of acetic acid takes place on the metal sites and that steam gets activated on the support. The acetic acid conversion was 100% during the entire experiment, but the H_2 yield dropped drastically after only 25 min of reaction time (though the activity of Pt supported by ZrO_2 was maintained for longer).

Table 5 provides a summary of works that have utilized noble metal-based catalysts for the SR of bio-oil. As evidenced, the loading of these metals on supports is very low leading to low availability of total metal sites. Therefore, in order to boost feed conversion, a higher reaction temperature (>600 °C) is required. Furthermore, a well-known disadvantage of noble metal catalysts is their high cost which limits practical utilization and industrial implementation. The combination of noble and transition metals could ameliorate this limiting factor and also help to augment the resistivity towards coking.

5.2. Transition Metal-Based Catalysts

Transition metals have attracted great interest as catalysts for steam reforming reactions due to their low cost and good catalytic activity. As is well understood, the choice of support has a crucial role on the properties of the catalytic system, as it affects the dispersion of the active phase over the surface of the carrier, the stability shown by the catalytic system through the degree of interaction achieved between metal and support. Moreover, the support can influence the reaction pathway and the deposition of carbon [118]. For the SR of bio-oil in particular, the organic molecules are dissociatively adsorbed on metal sites, whereas H_2O molecules are adsorbed on the supporting metal oxide surface (e.g., Al_2O_3, MgO).

5.2.1. Ni-Based Catalysts

Ni is known to exhibit great capacity to break C–C and C–H bonds. For this reason, nickel is regarded as highly efficient for the SR of raw bio-oil, its aqueous fraction and oxygenate model compounds. This is demonstrated by numerous studies which have reported very high values for bio-oil conversion and H_2 selectivity [77,79,100]. Al_2O_3 is frequently used to support Ni catalysts due to its high surface area and high thermal and chemical stability [76,77,79]. It can also have a large influence on the stability of the catalyst, by enhancing the dispersion of the metals and providing active sites that are more accessible to the reactants. Chornet and co-workers [41,42,72,108,119] extensively studied the catalytic SR of bio-oil over various research and commercial Ni-based catalysts. Experiments on the steam reforming of bio-oil aqueous fraction over $Ni/\alpha\text{-}Al_2O_3$ at 825 °C, S/C = 4.92 and HSV = 126,000 h^{-1} have shown an initial hydrogen yield of about 90% (the remaining 10% being CH_4 and coke) which dropped by about 30% after 25 min of experiments due to partial deactivation by coking [41]. Support modified $Ni/MgO\text{-}Al_2O_3$ and $Ni/MgO\text{-}La_2O_3\text{-}Al_2O_3$ catalysts exhibited superior performance with higher hydrogen yields and significantly slower deactivation. Czernik et al. [120] compared the performance of commercial and laboratory prepared Ni-based catalysts during the SR of

raw bio-oil and reported H_2 yields up to 80% of the stoichiometry. This result was achieved at 850 °C, S/C = 5.8 and a CH_4 equivalent space velocity of 920 h^{-1}. The commercial naphtha reforming Ni-based C11-NK (Sud-Chemie) catalyst showed somewhat higher activity than four NREL prepared Ni-based catalysts and a remarkable stability on the yield of H_2 over a 18 h time-on-stream experiment. Despite this fact, catalyst deactivation due to the methanation of CO and the thermal cracking of complex bio-oil molecules was still a detectable problem. Generally, an increase of the Ni content in the catalytic system up to 10–15% increases the conversion of oxygenates, but attention should be paid, as very high Ni loadings lead to extensive sintering [121].

Table 5. Summary of the literature on bio-oil steam reforming using noble metal-based catalysts.

Type of Feed [1]	Catalyst	Prep. Method	Experimental Conditions	Comments	Ref.
acetic acid, acetone, separately	5% Ni, 0.5% Rh supported on $CaO{\cdot}2Al_2O_3$ and $12CaO{\cdot}7Al_2O_3$	wet impregnation	fixed bed quartz reactor; 0.05 g catalyst diluted with 0.10 g quartz particles; GHSV = 34,500 h^{-1} for acetic acid & 28,500 h^{-1} for acetone; S/C = 3; P = 1 atm; T = 550–750 °C	$Ni/CaO{\cdot}2Al_2O_3$ showed highest H_2 yield and $Rh/CaO{\cdot}2Al_2O_3$ showed highest coking resistance.	[63]
acetic, propionic, butyric acid, separately and mixture (HAc:HPr:HBu 6:1:3)	5% Ru, Pd, Rh, Pt, Ni supported on Al_2O_3	incipient wetness impregnation	fixed bed quartz reactor; 200 mg catalyst; GHSV = 25,000 h^{-1}; S/C = 9; T = 300–600 °C	Activity decreased in the order of Ru > Pd ~ Rh > Pt > Ni.	[117]
acetic acid	1% Pt, 1% Pd, 0.5% Rh, 1 and 5% Ru, 17% Ni supported on Al_2O_3, 15% La_2O_3/Al_2O_3, 15% MgO/Al_2O_3 and 30% CeO_2/Al_2O_3	wet impregnation	fixed bed micro-reactor; 100 mg catalyst; flow rate: 290 cm^3/min; S/C = 4; P = 1 atm; T = 550–800 °C	Ni- and Ru-based catalysts present higher activity and selectivity (approximately 100% at 750 °C). Ru catalysts show long-term stability (for ~35 h).	[81]
acetic acid, phenol, acetone, ethanol, separately and raw bio-oil	1% Pt, Pd and Rh/Al_2O_3 and CeO_2–ZrO_2 (15/85%)	incipient wetness impregnation	fixed bed quartz reactor; 100–200 mg catalyst; GHSV = 3090 h^{-1}; S/C = 5–10.8; T = 650–950 °C	Order of activity: 1% $Pd\text{-}Al_2O_3$ < 1% $Pt\text{-}Al_2O_3$ < 1% $Pd\text{-}CeZrO_2$ < 1% $Rh\text{-}Al_2O_3$ < 1% $Pt\text{-}CeZrO_2$ < 1% $Rh\text{-}CeZrO_2$.	[70]
acetic acid	5% Ni, 0.5% Rh/CeO_2–ZrO_2 (15/85)	wet impregnation	fixed bed quartz reactor; 50 mg of catalyst diluted with 100 mg quartz; GHSV = 34.500 h^{-1}; S/C = 3; P = 1 atm; T = 550–750 °C	Ni and Rh metals enable the reforming reactions to proceed with high rates even at 650 °C. Lowest coke deposition for the Rh catalysts.	[64]
acetic acid	0.5% Pt/ZrO_2	wet impregnation	fixed-bed reactor; 50 mg catalysts; WHSV = 9.0 h^{-1}; GHSV = 160,000 h^{-1}; S/C = 5; T = 500–700 °C	Pt was essential for the SR to proceed. ZrO_2 helped activate steam.	[68]
acetic acid	0.5% Pt/ZrO_2	wet impregnation	fixed bed reactor; 50–200 mg catalysts; SV = 40,000–160,000 h^{-1}; S/C = 5; T = 600–800 °C	Pt/ZrO_2 was initially active but then deactivated rapidly due to the blockage of the Pt-related active sites.	[69]
acetic acid	0.5% Pt/ZrO_2	wet impregnation	fixed bed reactor; 10–50 mg catalysts; GHSV = 320,000 or 1,600,000 h^{-1}; S/C = 5; T = 400–700 °C	H_2O activated on ZrO_2 to create additional surface hydroxyl groups.	[95]

[1] aqueous solution of every model compound is used as feedstock.

Another common feature in the catalyst design is the incorporation of additives or promoters. Examples include the addition of an alkali or alkaline earth metals, often in high surface area supports, such as Al_2O_3, in order to combine with adjacent catalytically active metal sites for SR [122,123]. As CaO has good chemical and thermodynamic properties, it is considered an efficient solid sorbent that can aid enhanced activity [63,65,66,84]. A number of research works have also reported that the incorporation of K and La into the support, in small concentrations, can help prevent sintering and the formation of carbon [124]. In addition, the use of La as a promoter is known to aid the dispersion of the active metal and to promote the production of H_2 [72,74,80,125]. Galdamez et al. [126] synthesized Ni/Al_2O_3 catalysts using co-precipitation and investigated the extent to which the loading of La_2O_3 onto the catalysts affected the H_2 yield. They observed that during the non-catalytic SR, the yields of hydrogen and carbon dioxide were very low. Valle et al. [43] worked in a similar vein to the Galdamez group and concluded that the good performance of Ni/Al_2O_3 modified with La was due to its capacity for water adsorption, and thus enhancement of WGS reaction. Alternatively, MgO may be used to promote Al_2O_3 as the formation of a magnesium-aluminum spinel phase is thought to enhance the adsorption of steam [44,98,127]. Garcia et al. [41] studied the SR of the aqueous fraction of bio-oil using La and Mg modified alumina. The authors concluded that the presence of these modifiers enhanced steam adsorption and helped the gasification of surface carbon. Ca, Ce, Mg, Mn and Zn were also used as modifiers on Ni/Al_2O_3 catalysts by Yao et al. [128] in the SR of the aqueous fraction of bio-oil. $Ni/MgO\text{-}Al_2O_3$ catalyst showed the highest H_2 yield, equal to 56.46%, followed by $Ni/CeO_2\text{-}Al_2O_3$ (55.30%) and $Ni/ZnO\text{-}Al_2O_3$ (52.01%).

5.2.2. Other Transition Metal-Based Catalysts

Although Ni has been by far the most investigated metal [53,129,130], other transition metals can also provide high activity at moderate temperatures. Li et al. [49] examined the performance of mono, unsupported Mn, Fe, Co, Ni, Cu and Zn, and also, mono Mn, Fe, Co, Ni, Cu and Zn supported on Al_2O_3, in the SR of methanol, acetic acid and acetone. The authors showed that Ni- and Co-based materials had enhanced activity in comparison to Mn, Fe or Zn, due to the low capacity of the latter to break the chemical bonds of the organics or to activate steam. They also showed that the unsupported Cu-based catalyst was significantly less stable than Cu/Al_2O_3. However, the authors also observed that the unsupported Ni-based catalyst was more resistant towards coking in comparison with Ni/Al_2O_3.

Additionally, mesostructured materials, such as SBA-15 silica, are thought to constitute promising supporting materials because they can help to improve the dispersion of the metallic phase. This property is the result of their mesoporous structure, which allows metal particles to diffuse through the available channels. Thus, sintering may be avoided through the increased interaction achieved between the support and the active [131]. Vizcaíno et al. [84] investigated a novel application of Co-based catalysts supported on SBA-15 and Mg or Ca modified SBA-15 in the SR of ethanol. The authors were able to show that the use of these modifiers resulted in an improvement of the dispersion of the active phase, increased metal-support interaction, and enhanced the materials' basicity. Despite these improvements, ethanol conversion and H_2 production were clearly lower compared to analogous Ni catalysts. This was attributed to the higher reduction temperatures required for their activation. Megía et al. [65,66] also analyzed the effect of Ca addition to Co/SBA-15 in the SR of acetic acid. The authors observed that higher temperatures were necessary to activate the catalysts, which they attributed either to the stronger interaction between the active phase and the support or to the formation of a new Ca-Co compound. Additionally, the authors investigated the effect on the catalytic activity of the addition of Cu, Ag, Ce and Cr, i.e., Co-M/CaSBA-15 (M:Cu, Ag, Ce, Cr). These promoters not only helped obtain increased metallic dispersion and stronger metal-support interaction, but also increased the reducibility leading to higher acetic acid conversion. The Co-Ce/CaSBA-15 catalyst showed the highest conversion value and the highest reducibility. The addition of CeO_2

in the catalyst enhanced the population of oxygen vacancies and aided the dispersion of metal over the support. As a result, an improvement in the H_2 yield was observed and coke gasification and WGS reaction were promoted. However, it was also observed that Cu could not improve the yield of H_2, as it favored the decarboxylation of acetic acid rather than its SR. Regarding the role of Ag, it was found to improve catalytic performance, but it also promoted the formation of carbonaceous species. The performance of Co-Cr/SBA-did not differ much in comparison to the performance of Co-Ce/CaSBA-15, but the presence of Cr raises questions about the material's toxicity [132]. Generally, the characteristics of Co-based catalysts are similar to Ni-based systems, however, Co is susceptible to particle agglomeration [65,66,77,84,96].

Fe is one of the most commonly used metals due to its capacity to break the C—C bond however, it also shows poor reactivity and weak reducibility [98]. Cu-based catalysts can also break the C—H bond and are considered active for the SR of methanol, but do not have the capacity to scissor the C-C bond in acetic acid or acetone [56] Table 6 summarizes the experimental conditions and the catalysts used in the above studies.

5.3. Bimetallic Catalysts

Bimetallic systems are an effective way of combining the advantages of different active metals [65,66,97,99]. For instance, the incorporation of Ru or Rh as promoters in Ni-based systems has been shown to positively affect activity by helping the reducibility of Ni species [89,91]. Salehi et al. [134] tested Ru-Ni/Al_2O_3 and Ni/Al_2O_3 catalysts with different Ni contents for the SR of acetic acid. The maximum H_2 yield (85%, T = 950 °C) was obtained with the doped Ru-Ni catalyst.

The synergistic interaction between Ni and Co also shows high reforming activity and H_2 selectivity since Co favors the WGS reaction where Ni is less active [135]. Assaf et al. [76], investigated Ni-Co bimetallic catalysts with varied Ni and Co loadings and argued that Co helped reduce coke formation and enhance catalytic performance. Garcia et al. [41] carried out experimental work using the aqueous fraction of bio-oil. The catalytic systems tested comprised of Ni-Al_2O_3 modified with La and Mg and bimetallic Ni-Cr and Ni-Co. The best results were recorded for Cr-promoted and Co-promoted catalysts based on MgO-La_2O_3-Al_2O_3, because Cr and Co formed alloys with Ni and led to a lowering of the crystallite size. Cr and Co promoters were also shown to inhibit the coke formation reactions. Likewise, Pant et al. [78] synthesized Ni-Co catalysts, and showed that these were more active than conventional monometallic systems, because they did not favor the methanation or reverse WGS reactions and promoted the SR.

Wang et al. [73] studied Co-Fe unsupported catalysts with varied Co/Fe ratios in the SR process. The authors concluded that increasing the amount of Fe in the system negatively affected catalytic activity and stability, owing to the unstable adsorption of water on Fe surface, which inhibited the SR and WGS reactions. Mohanty et al. [136] carried out a detailed study on Cu-Zn catalysts and concluded that the incorporation of Zn improved the hydrogen yield and minimized the deactivation of the active sites on the catalyst. Finally, it has also been shown that the use of Ni-Cu alloys leads to enhanced catalytic activity and improved time-on-stream stability, in comparison to monometallic Ni-based catalysts [137,138]. Table 7 provides a summary of the literature on bio-oil steam reforming using bimetallic catalysts. As concluded from the above results, the formation of an alloy of two metals enhances the catalytic performance and coke resistance. The synergy of two metals strengthens metal support interaction and improves metal distribution as well as the entire properties of the catalyst.

Table 6. Summary of the literature on bio-oil steam reforming using transition metal-based catalysts.

Type of Feed [1]	Catalyst	Preparation Method	Experimental Conditions	Comments	Ref.
acetic acid, acetone, separately	25% Ni/Al_2O_3	incipient wetness impregnation	fixed bed quartz reactor; 0.2 g catalyst with equal amount of quartz; flow rate = 0.2 mL/min; LHSV = 12.1 h^{-1}; S/C = 6; P = 1 atm; T = 450–700 °C	Ni/Al_2O_3 was highly selective and stable after the suppression of the presence of the Ni species which strongly interacted with alumina resulting in the formation of by-products and coking.	[77]
acetic acid	18% Ni/Al_2O_3	commercial catalyst	fixed bed quartz reactor; 2 g catalyst; flow rate: 0.0336 mL/min; S/C = 2–3; P = 1 atm; T = 550–750 °C	H_2 yield was 76.4% of equilibrium. HAc conversion was 88.97% at 750 °C. Chemical looping reforming technology.	[79]
acetic acid	Ni/Al_2O_3 (Ni/Al 1:2), Ni/La_2O_3-Al_2O_3 (8 and 12% La)	co-precipitation	fluidized bed stainless steel reactor; flow rate: 1.84–2.94 g/min; GHSV = 13,000 h^{-1}; S/C = 5.58; T = 450–700 °C	yield of H_2 was 0.029 g/g acetic acid at 650 °C.	[126]
bio-oil aqueous fraction	10% Ni/a-Al_2O_3, 10% Ni/La_2O_3-a-Al_2O_3 (10% La)	wet impregnation	fluidized bed reactor; 0.10–0.45 g catalyst h/g bio-oil; GHSV = 8100–8140,300 h^{-1}; S/C = 12; P = 1 atm; T = 600–800 °C	La_2O_3 improves the H_2 yield and selectivity.	[43]
bio-oil aqueous fraction	Ni-based catalyst with dolomite (CaO-MgO) sorbent	commercial catalyst (Z417)	fixed bed quartz reactor; P = 1 atm; T = 550–650 °C	75% H_2 yield at 600 °C. Chemical looping technology (CO_2 capture).	[52]
acetic acid	17% Ni/γ-Al_2O_3 promoted with 15% Mg, La, Cu, and K	incipient wetness impregnation	fixed bed reactor system; 0.044 mL catalyst volume; S/C = 5.3; P = 1 atm; T = 450–600 °C	With Mg promoter ~100% of H_2 and carbon selectivity, even at 450 °C.	[80]
acetic acid phenol	15% Ni/Ash (SiO_2, Al_2O_3, Fe_2O_3, CaO, MgO, K_2O, and Na_2O)	wet impregnation	fixed-bed reactor; 1 g catalyst; WHSV = 4 h^{-1}; S/C = 9.2, 7.5, 5, 2.5, 1; T = 500–800 °C	98.4% acetic acid conversion and 83.5% phenol conversion, 85.6% H_2 yield from acetic acid SR and 79.1% H_2 yield from phenol SR, at 700 °C.	[125]
acetic acid	15% Ni-MgO/γ-Al_2O_3 (1,5,10% Mg)	wet impregnation	fixed bed quartz reactor; 100 mg of catalyst; flow rate = 0.25 mL/h; T = 500–600 °C	15% Ni-5% Mg/Al_2O_3 more selective for H_2 production with high stability and sintering resistance ability.	[127]
bio-oil aqueous fraction	Ni/Al_2O_3, Ni/MgO-Al_2O_3 Ni/MgO-La_2O_3-Al_2O_3 (15% Ni, and mole ratios of Mg/Ni = 1, Ni/La = 8)	wet impregnation	fixed bed microreactor/molecular beam mass spectrometer; 3 cm high catalyst with quartz chips; GHSV up to 126,000 h^{-1}; S/C = 4.92–11; T = 825–875 °C	Mg and La promoters enhanced steam adsorption.	[41]
raw bio-oil	Ni-based naphtha	commercial catalyst (C11-NK)	fluidized bed reactor; flow rate = 120–300 g/h; GHSV = 700–1000 h^{-1}; S/C = 7, 9; T = 800–850 °C	Yields approached the theoretically possible for stoichiometric conversion at 850 °C.	[42]

Table 6. *Cont.*

Type of Feed [1]	Catalyst	Preparation Method	Experimental Conditions	Comments	Ref.
raw bio-oil	Ni/ZrO_2, Ni/Al_2O_3 (0, 5.6, 10.7, 14.1, 18% Ni)	wet impregnation	fixed bed stainless steel reactor; 0.2 g catalyst; WHSV = 13 h^{-1}; S/C = 5; T = 850 °C	61% H_2 yield with 5.6% and 10.7% Ni/ZrO_2 at 850 °C, 65% H_2 yield with 14.1% Ni/Al_2O_3 at 850 °C.	[133]
bio-oil aqueous fraction	Ni/CeO_2-ZrO_2 (5, 7,5, 10, 12% Ni and 5, 7,5, 10% Ce)	co-precipitation and wet impregnation	fixed bed quartz reactor; S/C = 4.9; P = 1 atm; T = 450–800 °C	69.7% H_2 yield with 12% Ni/7.5% Ce-Zr-O at 800 °C.	[45]
acetic acid	Ni/Ce-Zr-O (0, 2.5, 5, 7.5, 10, 12% Ni and 0, 2.5, 5, 7.5, 10% Ce)	co-precipitation and wet impregnation	fixed bed quartz reactor; 3 g catalyst; LHSV = 3–11,5 h^{-1}; S/C = 0–3.5; P = 1 atm; T = 500–900 °C	83.4% H_2 selectivity and 0.39% CH_4 selectivity with 12% Ni/7.5% Ce-Zr-O at 650 °C; S/C = 3; LHSV = 2.8 h^{-1}.	[59]
acetic acid	15% Ni/CeO_2-ZrO_2-CaO with different Ce/Zr/Ca ratios of 0.2:1:5, 1:1:5, 1.2:1:5, and1.5:1:5	sol−gel and wet impregnation	fixed bed reactor; 2 g catalyst; flow rate = 0.96 mL/h; LHSV = 0.48 $mLg^{-1}h^{-1}$; S/C = 4; T = 550–750 °C	83% H_2 yield with $Ni/Ce_{1.2}Zr_1Ca_5$ catalyst at 550 °C; Sorption enhanced steam reforming.	[57]
acetic acid	Ni/ATC (Attapulgite Clay)	precipitation, wet impregnation, and mechanical blending	fixed bed stainless steel reactor; 3 g catalyst; flow rate = 14 mL/h; P = 1 atm; T = 550–650 °C	83% H_2 yield with precipitation method synthesized catalysts at 650 °C.	[75]
ethanol	7% Ni, 7% Co supported on bare SBA-15 and on Mg or Ca-modified SBA-15	hydrothermal method for SBA-15, incipient wetness impregnation	fixed bed reactor; 100 mg of catalyst; flow rate: 0.075 mL/min ($WHSV_{EtOH}$ = 16.8h^{-1}); GHSV = 22,300 h^{-1}; P = 1 atm; T = 600–700 °C	100% EtOH conversion, 90.3 mol % H_2 selectivity and 6.7 wt. % coke deposition at 700 °C with Ni/Ca/SBA-15 catalyst. Mg and Ca in Co/SBA-15 promote metal properties (dispersion and interaction) in greater degree than in Ni/SBA-15.	[84]
acetic acid	Co-M/SBA-15 (Co: 7%; M: 2% of Cu, Ag, Ce and Cr)	hydrothermal method for SBA-15, incipient wetness impregnation	fixed bed stainless steel reactor; WHSV = 30.1 h^{-1}; GHSV = 11,000 h^{-1}; S/C = 2; P = 1 atm; T = 600 °C	70 mol % H_2 selectivity at 600 °C with Co-Cr/SBA-15.	[65]
acetic acid	Co/SBA-15 and Co-M/CaSBA-15 catalysts (Co: 7%; M: 2% of Cu, Ag or Ce)	hydrothermal method for SBA-15, incipient wetness impregnation	fixed bed reactor; WHSV = 30.1 h^{-1}; S/C = 2; P = 1 atm; T = 600 °C	71.8% H_2 yield and 99% conversion at 600 °C with Co-Ce/CaSBA-15. Cu improved the decarboxylation reaction of acetic acid and did not improve H_2 production. Ag enhanced catalytic performance and decreased coke deposition. Ce improved further Co dispersion.	[66]
phenol	Fe/50Mg-50Ce-O (1, 2.5, 5,10% Fe)	sol–gel and incipient wetness impregnation	0.15 g catalyst in 0.15 g of SiO_2 GHSV = 80,000 h^{-1} T = 600–700 °C	5% Fe/50Mg-50Ce-O catalyst the most active in terms of H_2 yield at 700 °C. Coke deposition increased with increasing Fe loading	[98]

[1] aqueous solution of every model compound is used as feedstock.

Table 7. Summary of the literature on bio-oil steam reforming using bimetallic catalysts.

Type of Feed [1]	Catalyst	Preparation Method	Experimental Conditions	Comments	Ref.
glycerol, syringol, n-butanol, m-xylene, m-cresol, furfural mixture (1:1:1:1:1:1)	14% Ni/25% CeO_2-Al_2O_3; 1% Me-14% Ni/25% CeO_2-Al_2O_3 (Me = Rh, Ru)	wet impregnation	fixed bed reactor; 400 mg of catalyst in 3.6 g of SiC; WHSV = 21.15 h^{-1}; S/C = 5; P = 1 atm; T = 700–800 °C	Ru or Rh promoters enhanced the activity of the Ni/CeO_2-Al_2O_3 catalysts by aiding the reducibility of Ni.	[89]
acetone	12% Ni/15% La_2O_3-Al_2O_3; 1% M-12% Ni/15% La_2O_3-Al_2O_3 (M = Pt or Cu)	wet impregnation	fixed bed quartz reactor; 0.5 cm^3 of catalyst diluted with SiC at a volume ratio of 3:1; GHSV= 10,180 h^{-1}; P = 1 atm; T = 500–700 °C	The activity order of H_2-rich syngas Pt-Ni/La_2O_3-Al_2O_3 > Cu-Ni/La_2O_3-Al_2O_3.	[97]
acetol	Ni/Al_2O_3 (Ni/Al = $\frac{1}{2}$), Ni/La_2O_3-Al_2O_3 (4, 8 and 12 wt. % La), Ni-Co/Al_2O_3 (Co/Ni = 0.025 and 0.25)	co-precipitation	fluidized-bed stainless steel reactor; 2.27 to 8.52 g catalyst min/g acetol; GHSV = 22,323 to 5947 h^{-1}; flow rates up to 5 mL/min, S/C = 4.6; P = 1 atm; T = 450–650 °C	The activity order of syngas Ni/Al_2O_3 = Ni-Co/Al_2O_3 > Ni/La_2O_3-Al_2O_3.	[99]
acetic acid	20% Ni–10%Co/γ-Al_2O_3, 25%Ni–5%Co/γ-Al_2O_3		fixed bed reactor; 100 mg catalyst; flow rate = 0.25 mLh^{-1}; P = 1 atm; T = 500–600 °C	Co led to an inhibition of carbon deposition.	[76]
bio-oil aqueous fraction	Ni-Cr/MgO-La_2O_3-Al_2O_3; Ni-Co/MgO-La_2O_3-Al_2O_3 (15% Ni, and mole ratios of Mg/Ni = 1, Ni/La = 8, Ni/Cr = 3, and Ni/Co = 3)	impregnation	fixed bed micro-reactor/molecular beam mass spectrometer system; 3 cm high catalyst with quartz chips; GHSV up to 126,000 h^{-1}; S/C = 4.92–11; T = 825–875 °C	Co and Cr additives reduce coke formation. Ni-Cr/MgO-La_2O_3-Al_2O_3 show the best results.	[41]
acetone	8% Ni/$MgAl_2O_4$, 4% Co-4%, Ni/$MgAl_2O_4$, 8% Co/$MgAl_2O_4$	incipient wetness impregnation	fixed bed reactor; 100 mg catalyst; W/F = 70.6 g_{cat} min $g_{acetone}{}^{-1}$; T = 550–750 °C	Coke oxidation was favored on Co-containing catalysts.	[96]
acetic acid	Ni-Co (20:80%), Ni–Co/CeO_2-ZrO_2 (15:60:10:15%), Ni/La_2O_3-Al_2O_3 (17% Ni,15% La)	co-precipitation and impregnation	fixed bed quartz reactor; 3 g catalyst; flow rate: 0.5–1.12 mL/min; GHSV = 79.6 g-cat h/mole acetic acid; P = 1 atm; T = 550–700 °C	The unsupported Ni–Co exhibited the highest activity and H_2 yield.	[78]
acetic acid	Ni and Co (range from 1:0 to 0:1)	co-precipitation	fixed bed quartz reactor; 1 mL catalyst with equal amount of quartz; LHSV = 5,1 h^{-1}; S/C = 7.5; P = 1 atm; T = 250–550 °C	Catalytic activity improved by increasing the content of Co. The best results were achieved when the Ni to Co ratio was 0.25:1.	[7]
acetic acid	Co-Fe (pure Co, Co/Fe = 0.5, Co/Fe = 2, and pure Fe)	co-precipitation	fixed-bed reactor; 0.3 g catalyst with quartz sand; LHSV = 4 h^{-1}; S/C = 9.2; P = 1 atm; T = 350–600 °C	Catalyst activity increased with increasing Co content. The conversion of acetic acid using the pure Co catalyst was 100%; the H_2 yield was 96%. These values were achieved at 400 °C.	[73]

[1] aqueous solution of every model compound is used as feedstock.

5.4. Perovskite Type Catalysts

Perovskite type oxides (Figure 5) have recently attracted considerable attention as potential catalysts for reforming reactions. Perovskites are mixed oxides with distinctive structural features and high redox properties. Their general formula isABO_3, in which A is a metal such as an alkali, alkaline, lanthanide or rare earth acting as a skeleton support,

while B is generally a transition metal such as Ni, Fe, Co, Cu, or Mn. The B site particularly, is a cation with a coordination number of six and it is the central site of structure [62]. Due to the great flexibility of the crystal lattice structure, partial substitution of cations in A and B position by other elements of a similar size can be achieved, resulting in significant changes to the catalyst's properties [61,71]. In addition, perovskites combine both high loadings of metals and high dispersion, preventing the agglomeration of metal ions incorporated in their lattice. In addition to the small metal particle size, perovskites can retain their structure even at high temperatures, leading to good activity and thermal stability. As a result, the structure of perovskites has more active sites, increased mobility of oxygen ion vacancies and resistance to coke deposition [139].

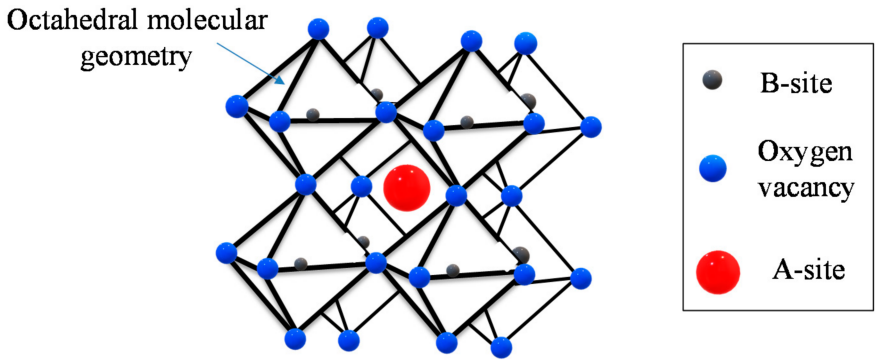

Figure 5. Perovskite structure ABO_3.

Liu et al. [62] compared the activity of $LaNiO_3$ and $LaNi_{0.8}M_{0.2}O_3$ perovskites substituted in the B site with Fe, Co, Mn, and Cu on the SR of acetic acid and showed that activity followed the order: $LaNi_{0.8}Fe_{0.2}O_3$ > $LaNi_{0.8}Co_{0.2}O_3$ > $LaNiO_3$ > $LaNi_{0.8}Mn_{0.2}O_3$ > $LaNi_{0.8}Cu_{0.2}O_3$. In another work [61] the same authors also studied a series of Fe-doped $LaNiO_3$ perovskites with different Ni/Fe ratios and concluded that despite $LaNiO_3$ showing higher activity for hydrogen production, the Ni-Fe bimetallic perovskites were more stable during the SR process. Among the partial substituted perovskites that have been examined, $LaNi_{0.8}Fe_{0.2}O_3$ demonstrated the best synergy between Ni and Fe. The coking resistance of the perovskite was also effectively improved due to Fe-doping. In a more recent work, Liu et al. [139] used $La_{0.8}M_{0.2}Ni_{0.8}Fe_{0.2}O_3$ perovskites substituted in the A site with Ca, Ce and Zr and showed that the $La_{0.8}Ce_{0.2}Ni_{0.8}Fe_{0.2}O_3$ having stronger surface basicity and increased oxygen adsorption capacity was more active and stable.

Resende et al. [67] examined $LaNiO_3$, $LaPrNiO_3$ and $LaSmNiO_3$ perovskites as precursors for catalysts in the SR of acetic acid. The products formed on the tested catalysts differed only in terms of selectivity. The substitution with Pr and Sm only marginally affected the catalytic performance. Li et al. [71] also concluded that Ce substitution enhanced the interaction between metal and support, promoted the WGS reaction and improved the resistance to the deposition of coke. Transmission electron microscopy (TEM) showed that the precursors were successfully synthesized (Figure 6).

The average H_2 yield and acetic acid conversion were 90 and 95%, respectively, when the $La_{0.9}Ce_{0.1}NiO_3$ perovskite was used. Similarly, Junior et al. [82] evaluated the effect of Ca content on the activity and hydrogen production in the SR of acetic acid. The results showed that the presence of Ca in the perovskite enhanced hydrogen yield by promoting the WGS reaction and limiting the ketonization reaction. Chen et al. [47] investigated the effects of the K substitution on Mn-based perovskite type catalysts and compared them to commercial Ni/ZrO_2. The results showed that the $La_{0.8}K_{0.2}MnO_3$ catalyst had a higher catalytic activity, with a hydrogen yield of 72.5%, however deactivation was an issue. A summary of the literature on bio-oil steam reforming using perovskite type catalysts is illustrated in Table 8.

5.5. Effect of Catalyst Synthesis Methods

As is well understood, the choice of the catalyst synthesis method can have a major impact on performance, as it regulates the dispersion of the active phase and the interaction between metal and support. In addition, it can also affect the carbon formation and, thus, the stability of the system [101,140]. As a consequence, a plethora of different methods have been employed to synthesize catalysts in an effort to enhance their properties and increase their activity. Wet or dry (incipient wetness) impregnation, is commonly used to load the metal species onto the supporting materials, owing to their simplicity. Nabgan et al. [141] investigated the synergetic effects between Ni and Co, in the SR of acetic acid using La_2O_3 as support; the catalysts were synthesized using the wet impregnation technique. However, although the dispersion of the active phases was high, carbon deposition was also heavy. Similarly, Valle et al. [142] attributed the deactivation of a Ni/La_2O_3-Al_2O_3 in the SR of raw bio-oil, prepared by the incipient wetness impregnation method, to the formation of encapsulating and filamentous coke. The smaller formation of encapsulating coke was attributed to the oxygen present in bio-oil, which was absorbed on the Ni sites, though the filamentous coke deactivating effect was the blockage of the catalyst pores.

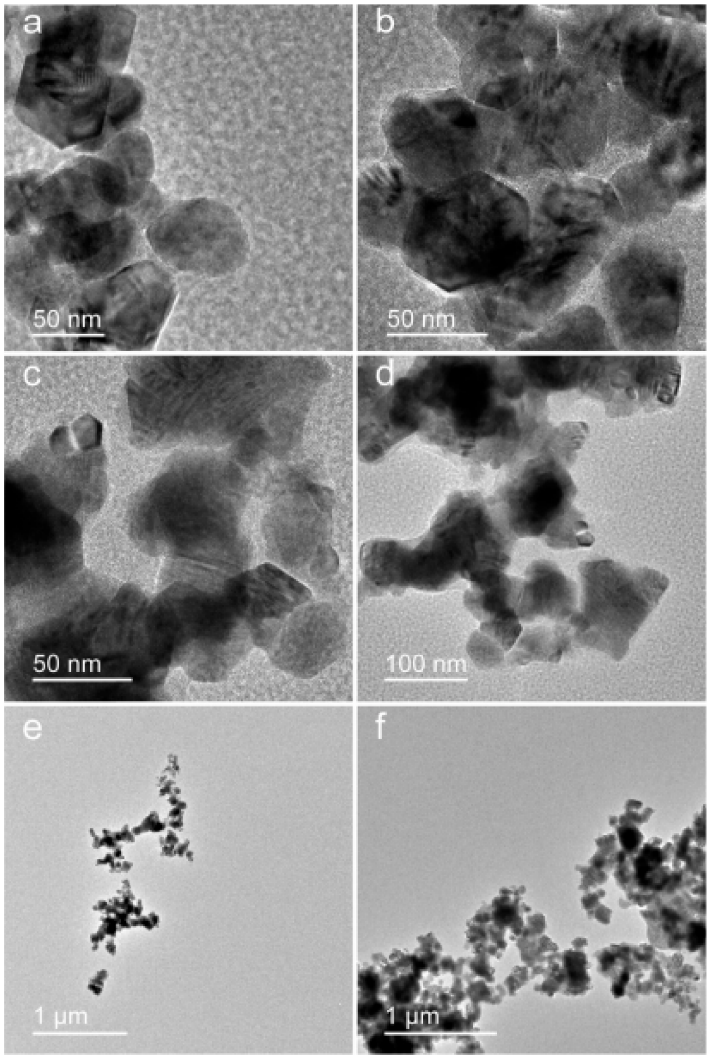

Figure 6. TEM images of different perovskites: (**a**) $LaNiO_3$; (**b**) $La_{0.95}Ni_{0.05}NiO_3$; (**c**) $La_{0.9}Ce_{0.1}NiO_3$; (**d**,**f**) $La_{0.8}Ce_{0.2}NiO_3$; and (**e**) $La_{0.7}Ce_{0.3}NiO_3$. Reproduced with permission from [71]. Copyright Elsevier, 2021.

Table 8. Summary of the literature on bio-oil steam reforming using perovskite type catalysts.

Type of Feed	Catalyst	Prep. Method	Experimental Conditions	Comments	Ref.
acetic acid	$LaNiO_3$ and $LaNi_{0.8}M_{0.2}O_3$ (M = Fe, Co, Mn, Cu)	sol-gel	fixed bed reactor; 0.2 g catalyst; GHSV = 34,736 g of feed/(g catalyst h); S/C = 2; P = 1 atm; T = 650 °C	Activity, during the chemical looping SR followed the order: $LaNi_{0.8}Fe_{0.2}O_3$ > $LaNi_{0.8}Co_{0.2}O_3$ > $LaNiO_3$ > $LaNi_{0.8}Mn_{0.2}O_3$ > $LaNi_{0.8}Cu_{0.2}O_3$.	[62]
acetic acid	$LaNi_xFe_{1-x}O_3$ (x = 0, 0.2, 0.4, 0.6, 0.8 and 1)	sol-gel	fixed bed reactor; 0.2 g catalyst; flow rate = 35 mL/min; S/C = 3; P = 1 atm; T = 600 °C	Perovskites doped with Fe contained more lattice oxygen with$LaNi_{0.8}Fe_{0.2}O_3$ exhibits the best synergistic effect and achieves the highest H_2/CO for H_2-rich syngas production. Chemical looping steam reforming process.	[61]
acetic acid	$LaNi_{0.8}Fe_{0.2}O$, $La_{0.8}M_{0.2}Ni_{0.8}Fe_{0.2}O_3$ (M = Ca, Ce and Zr)	sol-gel	fixed bed reactor; 0.25 g catalyst; S/C = 2; P = 1 atm; T = 600 °C	Doping on A-site with basic metals improves redox properties of the perovskite. Ce-doped oxygen carriers showed improved catalytic performance.	[139]
acetic acid	$LaNiO_3$ $LaPrNiO_3$ $LaSmNiO_3$	precipitation	fixed bed reactor 10 mg of catalyst diluted with 150 mg of SiC; flow rate = 400 mL/min; S/C = 3; P = 1 atm; T = 600 °C	Catalytic performance was affected only marginally by the addition of Pr and Sm.	[67]
acetic acid	$La_{1-x}Ce_xNiO_3$(x = 0, 0.05, 0.1, 0.2, and 0.3)	citrate	fixed bed reactor; 500 mg catalyst; flow rate = 4 mL/h; S/C = 3; P = 1 atm; T = 650, 700, 750 °C	Ce substitution of La affects the properties of perovskites. $La_{0.9}Ce_{0.1}NiO_3$ showed improved performance with H_2 yield of 90% and acetic acid conversion of 95%.	[71]
acetic acid	$La_{1-x}Ca_xNiO_3$(x = 0, 0.15, 0.30 and 0.50)	citrate	fixed bed reactor; 10 mg of catalyst diluted with 150 mg of SiC; flow rate = 0.25 mL/min; S/C = 3; P = 1 atm; T = 400–700 °C for $LaNiO_3$ and 600 °C for Ca-containing catalysts	The presence of CaO promoted the H_2 production and the WGS reaction.	[82]
bio-oil aqueous fraction	$La_{1-x}K_xMnO_3$(x = 0, 0.1, 0.2, 0.3)	sol-gel	fixed bed reactor; WHSV = 12 h^{-1}; S/C = 3; P = 1 atm; T = 600–800 °C	K substitution helped obtain a higher surface area for $LaMnO_3$. H_2 yield of 72.5% was recorded for $La_{0.8}K_{0.2}MnO_3$.	[47]

5.6. Effect of Catalyst Synthesis Methods

As is well understood, the choice of the catalyst synthesis method can have a major impact on performance, as it regulates the dispersion of the active phase and the interaction between metal and support. In addition, it can also affect the carbon formation and, thus, the stability of the system [101,140]. As a consequence, a plethora of different methods have been employed to synthesize catalysts in an effort to enhance their properties and increase their activity. Wet or dry (incipient wetness) impregnation, is commonly used to load the metal species onto the supporting materials, owing to their simplicity. Nabgan et al. [141] investigated the synergetic effects between Ni and Co, in the SR of acetic acid using La_2O_3 as support; the catalysts were synthesized using the wet impregnation technique. However, although the dispersion of the active phases was high, carbon deposition was also heavy. Similarly, Valle et al. [142] attributed the deactivation of a Ni/La_2O_3-Al_2O_3 in the SR of raw bio-oil, prepared by the incipient wetness impregnation method, to the formation of encapsulating and filamentous coke. The smaller formation of encapsulating coke was attributed to the oxygen present in bio-oil, which was absorbed on the Ni sites, though the filamentous coke deactivating effect was the blockage of the catalyst pores.

Wang et al. [75] prepared Ni catalysts supported on attapulgite (ATC) using the precipitation, wet impregnation and mechanical blending techniques and studied the catalytic SR of acetic acid. The authors concluded that the interaction between the Ni species and the ATC support was strong (for the samples prepared via precipitation), which was beneficial for catalytic activity and stability. Similarly, Zhang et al. [143] examined the SR of acetic acid using Ni-Co/MgO catalysts, synthesized using co-precipitation and wet impregnation. The catalyst prepared via wet impregnation showed decreased H_2 yield and were less stable due to significant coke deposition.

Catalyst synthesis via the sol-gel process is also commonly employed as it provides the means to control the surface and textural properties [47,62]. As the process is a wet chemical technique, it is also known as chemical solution deposition [61,139].

The hydrothermal method has the significant advantage of helping the self-assembly of products by taking advantage of the solubility of precursors in hot water (or organic solvent) under increased pressure [101]. Bizkarra et al. [90] investigated Zeolite L as catalyst support, during the SR of a mixture of bio-oil and bio-glycerol. The catalysts showed improved catalytic performance, high H_2 yields and resistance to deactivation during the steam reforming process.

In recent years ultrasonic agitation has also been employed during catalyst preparation. Wu and co-workers [144] argued that this method can produce catalysts where the active phase is highly and homogeneously dispersed, with a strong degree of interaction between metal particles. These characteristics contributed to superior catalytic performance with enhanced stability during time-on-stream.

6. Catalyst Deactivation and Regeneration

6.1. Coke Formation

Bio-oil contains a range of oxygenated organic compounds which lead to the formation of carbon. This effect is more pronounced when reforming raw bio-oil. An excellent review, presenting issues related to coking in the processes of bio-oil upgrading, the properties of coke formed, the mechanism for coking and the methods developed for tackling it has been provided by Hu et al. [105].

Coke deposition is a rather complicated issue as it can arise from a combination of the polymerization, dehydration, and cracking reactions [114,145]. To study the effect that the molecular structure of different oxygenated compounds has on coking, model compounds are employed. The coke formed also has different properties, depending on the structures of the different feedstock [85,105]. Figure 7 depicts encapsulating coke, with aliphatic and higher aromatic nature, placed in the most superficial and inner layers, respectively, and filamentous coke with more carbonized structure and/or polyaromatic with low oxygenates content [146,147]. As is well understood, the nature of the deposited

carbon has a significant influence on catalytic performance, as amorphous carbon is easier to combust during reaction [105,148,149].

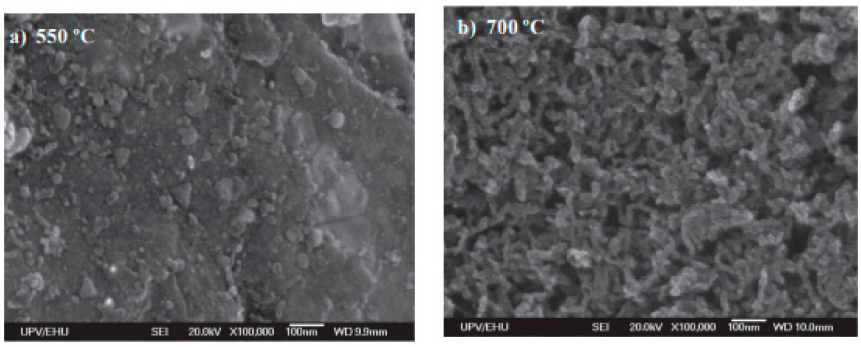

Figure 7. SEM images of coke deposits at 550 °C: (**a**) and 700 °C (**b**) under the same operating conditions. At 550 °C an amorphous carbon can be identified, and at 700 °C structures that are more filamentous can be identified. Reproduced with permission from [147]. Copyright Elsevier, 2021.

It is also known that increased unsaturation, molecular weight, and aromaticity of the feed lead to increased carbon deposition [106,150]. As known, lower C/H ratios indicate coke that is more aliphatic, while higher C/H ratios indicate coke that is more aromatic. For example, carbon formed during the SR of acetone has been shown to be less aromatic than that formed during the SR of acetic acid [105]. Li et al. [55] also examined the reforming of carboxylic acids and concluded that the nature and number of C-C bonds not only affected their reactivity, but also their propensity towards coke formation and its properties. Furthermore, the authors argued that the longer aliphatic chains increased the tendency towards coking; for example, the SR of acetic acid led to the formation of predominantly amorphous coke, while the reforming of heavier carboxylic acids resulted in the formation of fibrous carbon. Zhang et al. [58] also showed that the particular molecular structures had an important effect on coking. For example, the authors showed that methanol and formic acid had low propensity to form coke during their SR, as they lack aliphatic carbon chains. On the other hand, the significant, graphite-like, coke deposition observed during the SR of furfural and guaiacol comes about because of their π-conjugated ring structures [114]. In general, the presence of phenols and its derivatives (e.g., catechols, guaiacols and syringols), in raw bio-oil is undesirable, as these compounds polymerize into complex carbonaceous structures. Thus, such compounds are considered the main responsible substances for catalyst deactivation, but clogging of the reactor, pipelines and filters has also been observed [151].

The nature of the active metal not only affects the quantity of carbon deposition, but also its quality and location [56], and a large number of works show that the latter factors play a more significant role in catalyst deactivation than the amount [100,105]. Vagia et al. [64], studied the SR of acetic acid, using Ni- and Rh- based catalysts supported on CeO_2-ZrO_2, and showed that the almost negligible carbonaceous deposition on Rh catalysts can be attributed to the minimal affinity of Rh to coking and to the fast supply of oxygen to the metal interface. In contrast, the identification of coke even at very high temperatures (750 °C) over the Ni catalyst indicated that the quantity of oxygen transferred through the support vacancies at the perimeter of the metal crystallites was not sufficient to fully oxidize the coke deposits.

Thus, the physicochemical properties of the catalyst play a fundamental role in the coke formation mechanisms. Importantly, the catalyst should be able to provide ample adsorbed H_2O-derived species (i.e., OH and H), to minimize the impact of the reactions that lead to coke formation. This means that the adsorbed OH and H should possess surface mobility capable of reaching and reacting with the adsorbed hydrocarbon-derived species [105]. Thus, the use of appropriate supports is key for this process. For example, a number of works have shown that the SR ability of typical Ni-Al_2O_3 or Ni-SiO_2/Al_2O_3 systems can be significantly

improved when Ca and/or K are used as promoters [65,66,120,123]. Incorporating MgO to Al_2O_3 can also improve the adsorption and H_2O dissociation capacity of the catalytic system [72]. Vizcaíno et al. [84], in their studies on the SR of ethanol, used Mg- and Ca-modified Co or Ni/SBA-15 formulations, and were able to show that these promoters (i.e., Ca and Mg) helped lower coke deposition. It is noted that for Co-based catalysts this effect was more evident using Mg, and for the Ni-based catalysts this effect was more evident by the addition of Ca.

Moreover, a key strategy for coke minimization is the enhancement of the adsorption of steam which facilitates the gasification of coke precursors. Additionally, slowing down or minimizing cracking, deoxygenation, and dehydration of adsorbed intermediate, i.e., the surface reactions leading to the formation of the coke precursors, is also crucial [152,153].

The use of different reactor designs has also been studied in the attempt to eliminate coke with reports suggesting that the use of fluidized bed reactors can enhance coke gasification [104–106].

Temperature also plays an important role in the SR of bio-oil. When the reaction takes place at low temperatures, the incomplete cracking of the organics favors their polymerization to form carbon. High reaction temperatures, on the other hand, helps the cracking of high molecule-mass organics, and their ensuing SR. Moreover, higher temperatures also favor the gasification of coke precursors with steam or carbon dioxide [83,154].

6.2. Active Metal Sintering

In addition to coke formation, sintering, caused by the high temperatures and high pressures of steam used in the process, is another important cause for catalyst deactivation (Figure 8). Sintering occurs when the metallic particles (active phase) are enlarged during the reaction. As is well understood, sintering occurs through two basic mechanisms. The first involves the relocation of entire particles over the support and their conjugation with other, nearby particles. The other mechanism takes place through the migration of atoms over the support from one crystallite to a neighboring crystallite (Ostwald ripening) [47]. In effect, sintering lowers the number of active sites available to the reactants but also stipulates the formation of carbon (favored over larger metal particles).

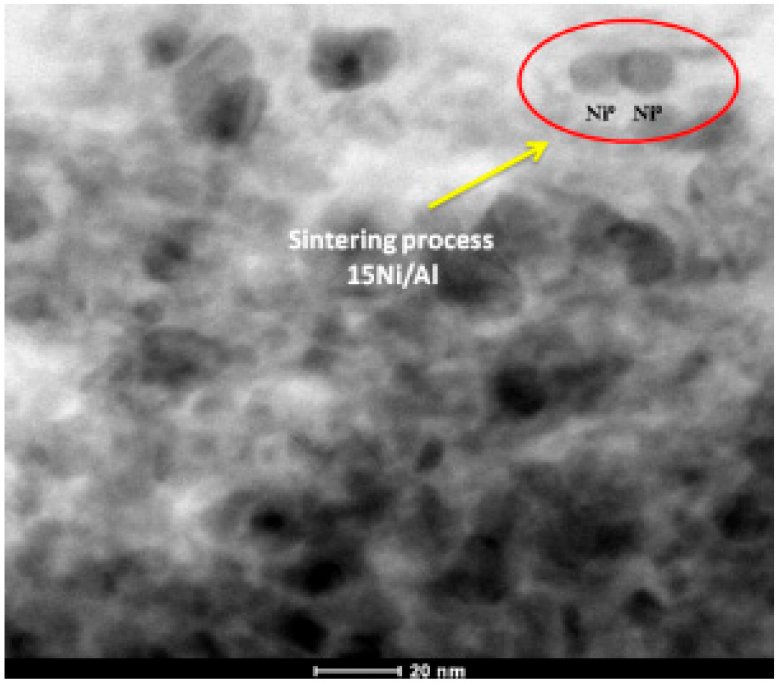

Figure 8. HRTEM image of 15% Ni/Al_2O_3 catalyst representing the sintering process. Reproduced with permission from [127]. Copyright Elsevier, 2021.

Sehested et al. [145,155–159] extensively studied the sintering of Ni-based catalysts in H_2O/H_2 model atmospheres and observed that the partial pressures of steam and hydrogen are of the utmost importance, as they probably control the rate at which sintering occurs. In particular, Ni supported in Al_2O_3 catalysts usually sinter when the environment is very hydrothermal, due to the extensive loading of Ni and the formation of $NiAl_2O_4$. However, the addition of small amounts of Mg, K, Ce or La can inhibit sintering by aiding the dispersion of the active metal, and by preventing the formation of the less active $NiAl_2O_4$ [88,128,160,161]. Zhao et al. [162] using a porous silica coated Ni/CeO_2-ZrO_2 catalyst and Pu et al. [163] using a series of Ni core-shell catalysts (with different shell species SiO_2, Al_2O_3, CeO_2, and TiO_2) were able to avoid sintering even at high reaction temperatures.

6.3. Active Metal Oxidation

The presence of O_2 in bio-oil may bring about the oxidation of the catalyst metallic species during steam reforming, which is subsequently detrimental to the catalytic activity and stability [150,164]. Nevertheless, the deactivation caused by active metal oxidation is not considered as serious an issue as coke formation or active metal sintering because of the use of inert carrier gases during the reaction.

6.4. Sulfur Poisoning

Sulfur, if present in the feed, is a severe poison which reduces the activity of the catalysts. All sulfur-containing compounds in the feed are converted into hydrogen sulfide (H_2S) at reforming conditions and then the sulfur atom in H_2S binds strongly to the metal (Equation (19)) (either transition or noble). As a result, even traces of sulfur in the feed lead to severe deactivation.

$$H_2S + Ni_{(surface)} \leftrightarrow Ni_{(surface)}\text{-}S + H_2 \quad (19)$$

Given this information, it is important to take into consideration the sulfur adsorption capacity of SR catalysts. Azad et al. [165] showed that the binding of sulfur to a compound such as CuO, added to noble metal-based catalysts, is more thermodynamically stable. Sato et al. [166] doped a Ni/MgO–CaO catalyst with WO_3 and showed good performance for reforming of naphthalene. $Ce_{0.8}Gd_{0.2}O_{1.9}$ has also been used to remove the sulfur on the catalyst as H_2S; this was achieved via a redox reaction [167]. Interestingly, sulfur poisoning can be used beneficially in order to decrease the coke formation. H_2S, in ppm levels, can be used to block the most active step sites, which are very active in whisker formation, and then the S-bonding can be reversed by treatment with H_2. This process allows the operation at a low S/C ratio [168,169].

Generally, a variety of physicochemical methods have been applied for the removal of the H_2S generated from industrial processes such as petroleum refining, natural gases, biogas processing and coal gasification [170–172]. Compared to naphtha which contains about 1.5% sulfur, bio-oil derived from the fast pyrolysis of biomass has a sulfur content in the range of 0.01–0.2% [142]. Thus, a desulfurization unit prior to the reformer may not be necessary for bio-oil feedstocks.

6.5. Catalyst Regeneration

A decrease in the cost of the reforming process can be achieved through catalyst regeneration and reuse. As stated above, carbon deposition constitutes the main deactivation mechanism in bio-oil reforming. Therefore, catalyst regeneration can be achieved if the coke can be removed. Combustion is a simply operated and highly efficient method which is commonly used for this purpose. In addition, combustion not only can eliminate the coke on the catalyst surface, but can also provide heat for the SR.

Wu et al. [173] reported that a regenerated Ni/MgO-Al_2O_3 catalyst had similar performance to the fresh catalyst. Ochoa et al. [146] showed that the carbonization structure and oxygen content affects the temperature at which combustion occurs, but also the heating

value of coke. Filamentous coke, which has higher structure of carbonization and lower oxygen content than encapsulating coke, requires high combustion temperature. Montero et al. [87] showed that the Ni/La_2O_3-Al_2O_3 catalyst undergoes partial Ni sintering in an ethanol reforming reaction-regeneration cycle system. Due to this, Oar-Arteta et al. [174] attempted to synthesize catalysts with metal spinel structure in order to obviate loss of metal activity in the regeneration process.

Coke can also be removed through gasification with air, oxygen or steam. However, more energy is needed and the coke removal rate is very slow compared with combustion [173,175].

7. Other Modified Reforming Techniques

As stated above, a higher S/C ratio is beneficial in attenuating coke formation during bio-oil steam reforming. However, this makes the process costly for the large-scale generation of hydrogen. For this reason, modified reforming methods for H_2 production from bio-oil have also been investigated.

7.1. Pyrolysis and in-Line Steam Reforming

Two-stage pyrolysis steam reforming has recently been proposed as an advanced technology for hydrogen generation. This process allows the valorization of both the whole bio-oil and gases from the pyrolysis step, avoiding the additional costs of transporting the bio-oil and also the bio-oil vaporization operational problems that occur during the one step bio-oil reforming process [176,177]. Incomplete vaporization and re-polymerization are some significant disadvantages of indirect bio-oil reforming that reduce its efficiency. As shown in Figure 9, pyrolysis and in-line reforming are carried out in a different reactor. The pyrolyzed derived product is directly fed into the reforming reactor and its thermal energy is utilized during reforming. The operating temperature is a key factor of the system as it affects the hydrogen regeneration significantly. Both processes have been optimized at different temperatures [42,178]. Therefore, pyrolysis process accompanied with in-line reforming has attracted much attention due to its considerable advantage over the biomass gasification, pyrolysis and bio-oil reforming.

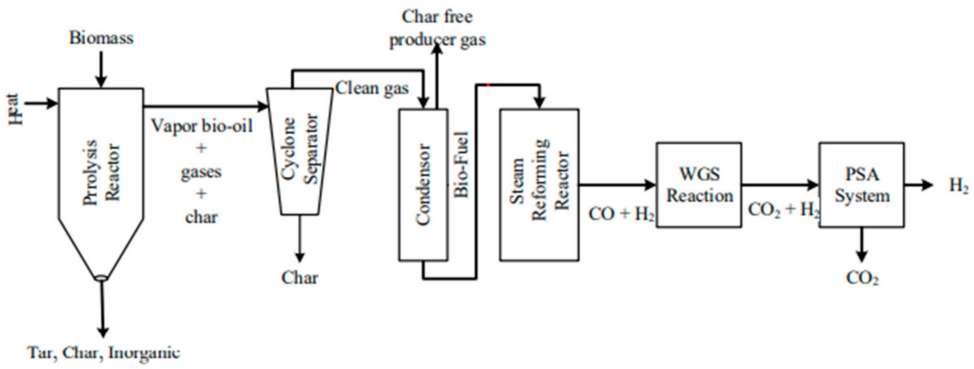

Figure 9. Schematic pathway of pyrolysis and in-line steam reforming process. Reproduced with permission from [26]. Copyright Elsevier, 2021.

Ma et al. [179] and Chen et al. [180] proposed a novel process for hydrogen production through a gas-solid simultaneous gasification process which was integrated into the two-stage pyrolysis SR process. This integrated process showed greatly increased H_2 yield and carbon conversion efficiency. The hydrogen obtained during this process was almost tar free.

7.2. Sorption Enhanced Steam Reforming (SESR)

Sorption enhanced steam reforming (SESR) has been proposed as a means to improve the purity of the hydrogen stream. Compared to the conventional SR process, SESR

involves a CO_2 sorption reaction which shifts the reaction equilibrium of the WGS reaction (Equation (2)) towards hydrogen, based on the Le Chatelier's principle. This also helps the removal of the produced CO. In general, a hydrogen feed of high CO_2 content is difficult to use for energy generation in fuel cells [181,182]. Thus, a sorbent such as CaO is added to the reacting system and reacts reversibly with CO_2 to reduce its concentration in the product stream according to the stoichiometry represented in Equation (20):

$$CaO + CO_2 \leftrightarrow CaCO_3 \tag{20}$$

The CO_2 removal by sorbents is an exothermic reaction. Therefore, the in-situ CO_2 capture is included in the process not only to clean the product steam of the non-combustible by-product, but also to decrease the whole reforming reaction temperature. The sorbent stability can be increased and the reforming operation becomes simpler by combining the sorbent and the catalyst in one catalytic system [57,183]. In addition to synthetic sorbents, natural sorbents such as dolomite (mainly MgO and CaO) and hydrotalcite have also been used [98,100]. The sorbent can also be regenerated and the high-purity CO_2 which is released in the regenerator can be reused. Thus, the SESR process is a promising pathway allowing low hydrogen production costs and a lower negative CO_2 output [44].

7.3. Chemical Looping Steam Reforming (CLSR)

Chemical looping steam reforming (CLSR) is an advanced auto-thermal reforming technology which has received appreciable attention during recent years. It has the abilities to reduce the hydrogen production costs, to utilize waste energy and to decrease the environmental impact. However, the complex reaction between an oxygen carrier and bio-oil may constrain its development [61]. CLSR couples the endothermic steam reforming and the exothermic partial oxidation of the reforming fuel (Equation (21)) by alternating fuel feed and oxidant feed, usually air. In partial oxidation, the substrate is oxidized with oxygen and releases heat, which in turn balances the energy required for the steam reforming process.

$$\text{(Substrate) } C_nH_mO_k + \text{air} \rightarrow \text{Carbonoxides} + H_2 + N_2 \tag{21}$$

In the fuel reactor, the bio-oil is partially oxidized into syngas by an oxygen carrier which is circulated between the fuel and air reactors. The oxygen carrier has a double role as it provides heat to the reactants within the reactor by oxidation reactions and also catalyzes the steam reforming and WGS reactions for hydrogen rich syngas formation. Hence, it is reduced from M_xO_y to $M_xO_{y-\delta}$ with less oxygen content. Then, the reduced oxygen carrier can be re-oxidized by air in an air reactor [139]. In general, a large amount of heat is transferred to the fuel reactor from the air reactor due to the exothermic nature of oxygen carrier oxidation process. Oxygen carriers can be simple metal oxides, mixed metal oxides and structured materials such as hydrotalcites and perovskites. Transition metals, such as Ni, Fe, Co and Mn have been widely studied owing to their higher natural abundance and higher sintering resistance than noble metals [62]. A well-designed CLSR process enhances the energy efficiency and may also produce a non N_2-diluted syngas with low heating demand [79].

8. Prospects, Directions and Conclusions

As the necessity for sustainable energy sources becomes increasingly important, the efficient production of renewable hydrogen becomes a challenge worth pursuing. The bio-oil produced by the fast pyrolysis of lignocelluloses is a product of higher energy density than the parent biomass which, being in liquid phase, can be transported in long distances easily and economically, allowing large-scale hydrogen production or the subsequent chemical synthesis of upgraded high density transportation biofuels (i.e., Fischer–Trospch synthesis) in central facilities.

The production of hydrogen or syngas through the catalytic SR of bio-oil is a key process in these large-scale energy scenarios and, as a result, has become a subject of extensive research during recent years. While in theory the steam reforming of bio-oil is entirely feasible and capable of producing high yields of hydrogen, in practice certain technological issues require further investigation and radical improvements before the commercialization of the process. Steam reforming is generally performed at middle to high reaction temperature, high S/C and low space velocity in order to maximize the formation of hydrogen and minimize the by-products. However, these parameters should be further investigated to simulate the conditions met in industrial operation. Also, the high chemical complexity of raw bio-oil does not readily allow a systematic approach on the maximization of hydrogen productivity while alleviating carbon deposition issues. Raw bio-oil cannot be completely vaporized and when heated leads to the formation of residual solids which accelerate catalyst poisoning at rates much higher than the usually examined model compounds. Aqueous phase bio-oil reforming suffers also from low H_2 yields and high coking rates and, as a result, model compound studies are used to simplify the catalytic reforming process, to determine how reactive the bio-oil components are, and to optimize H_2 production with the least catalyst coking. While some researchers examined hydrogen generation using a mixture of model compounds, further research is required on the reaction mechanisms and kinetics, which have not been yet fully understood and much work must be done to optimally treat the raw or aqueous bio-oil mixtures for efficient practical use.

The purpose of the present investigation is to provide the fundamental knowledge behind the technology of bio-oil steam reforming and to review the latest research outcomes and the recent progress on the development of the best suited catalysts and the most appropriate modified reforming techniques. Among the different catalysts which are being investigated, the most preferable seem to be the Ni-based due to their low cost, high abundance and good catalytic performance. For these, proper support modifications with basic oxides and active metal additions with alkali and alkaline earth metals have been reported to increase both the overall catalyst activity and the resistivity against coking. The properties of-and the interactions between the metal-based catalysts, the active phase additives and the support materials also require further study and clarification. Accordingly, further emphasis must be given to the research for catalysts with low cost, high activity and stability, strong regenerative ability and extensive operating lifetime for successful operation in the industrial conditions. Since catalyst deactivation is a major problem encountered during the steam reforming process, the mechanisms of coke formation and metal sintering should also be further investigated.

Author Contributions: A.P.: Investigation, Writing—Original Draft; N.D.C.: Conceptualization, Methodology, Writing—Review & Editing, Project administration; S.L.D.: Writing—Review & Editing; G.I.S.: Writing—Review & Editing; W.W.: Investigation, Writing—Review & Editing, Funding acquisition; G.L.: Writing—Review & Editing, Funding acquisition; V.G.P.: Writing—Review & Editing, Funding acquisition; M.A.G.: Writing - Review & Editing, Supervision, Project administration, Funding acquisition. All authors have read and agreed to the published version of the manuscript.

Funding: The authors are grateful to the project SYNAGRON, a joint RT&D project under Greece–China Call for Proposals launched under the auspices of the Ministry of Science and Technology (MOST) of the People's Republic of China and the Ministry of Development & Investments/General Secretariat of Research and Technology (GSRT) of the Hellenic Republic. China: National Key Research and Development Program, project code: 2017YFE0133300. Greece: European Regional Development Fund (ERDF) and National Resources (GSRT), project code: T7ΔKI-00388.

Institutional Review Board Statement: Not applicable.

Informed Consent Statement: Not applicable.

Data Availability Statement: Not applicable.

Conflicts of Interest: The authors declare no conflict of interest.

References

1. Zalasiewicz, J.; Waters, C.N.; Summerhayes, C.P.; Wolfe, A.P.; Barnosky, A.D.; Cearreta, A.; Crutzen, P.; Ellis, E.; Fairchild, I.J.; Gałuszka, A.; et al. The Working Group on the Anthropocene: Summary of evidence and interim recommendations. *Anthropocene* **2017**, *19*, 55–60. [CrossRef]
2. García-Olivares, A.; Solé, J.; Osychenko, O. Transportation in a 100% renewable energy system. *Energy Convers. Manag.* **2018**, *158*, 266–285. [CrossRef]
3. Aravani, V.P.; Sun, H.; Yang, Z.; Liu, G.; Wang, W.; Anagnostopoulos, G.; Syriopoulos, G.; Charisiou, N.D.; Goula, M.A.; Kornaros, M.; et al. Agricultural and livestock sector's residues in Greece & China: Comparative qualitative and quantitative characterization for assessing their potential for biogas production. *Renew. Sust. Energy Rev.* **2021**, *154*, 111821. [CrossRef]
4. Chen, C.; Yang, Z.; Hu, G. Signalling the cost of intermittency: What is the value of curtailed renewable power? *J. Clean. Prod.* **2021**, *302*, 126998. [CrossRef]
5. Siakavelas, G.I.; Charisiou, N.D.; AlKhoori, A.; AlKhoori, S.; Sebastian, V.; Hinder, S.J.; Baker, M.A.; Yentekakis, I.V.; Polychronopoulou, K.; Goula, M.A. Highly selective and stable Ni/La-M (M=Sm, Pr, and Mg)-CeO_2 catalysts for CO_2 methanation. *J. CO2 Util.* **2021**, *51*, 101618. [CrossRef]
6. Scharnberg, A.R.A.; Carvalho de Loreto, A.; Alves, A.K. Optical and Structural Characterization of $Bi_2Fe_xNbO_7$ Nanoparticles for Environmental Applications. *Emerg. Sci. J.* **2020**, *4*, 11–17. [CrossRef]
7. Feistel, R.; Hellmuth, O. Relative Humidity: A Control Valve of the Steam Engine Climate. *J. Hum. Earth Future* **2021**, *2*, 140–182. [CrossRef]
8. Liu, J.; He, Y.; Ma, X.; Liu, G.; Yao, Y.; Liu, H.; Chen, H.; Huang, Y.; Chen, C.; Wang, W. Catalytic pyrolysis of tar model compound with various bio-char catalysts to recycle char from biomass pyrolysis. *BioResources* **2016**, *11*, 3752–3768. [CrossRef]
9. Douvartzides, S.L.; Charisiou, N.D.; Papageridis, K.N.; Goula, M.A. Green diesel: Biomass feedstocks, production technologies, catalytic research, fuel properties and performance in compression ignition internal combustion engines. *Energies* **2019**, *12*, 809. [CrossRef]
10. Papageridis, K.N.; Charisiou, N.D.; Douvartzides, S.; Sebastian, V.; Hinder, S.J.; Baker, M.A.; AlKhoori, A.A.; AlKhoori, S.I.; Polychronopoulou, K.; Goula, M.A. Continuous selective deoxygenation of palm oil for renewable diesel production over Ni catalysts supported on $Al_2O_3$and La_2O_3-Al_2O_3. *RSC Adv.* **2021**, *11*, 8569–8584. [CrossRef]
11. Davda, R.R.; Shabaker, J.W.; Huber, G.W.; Cortright, R.D.; Dumesic, J.A. A review of catalytic issues and process conditions for renewable hydrogen and alkanes by aqueous-phase reforming of oxygenated hydrocarbons over supported metal catalysts. *Appl. Catal. B Environ.* **2005**, *56*, 171–186. [CrossRef]
12. Zhao, Z.; Situmorang, Y.A.; An, P.; Chaihad, N.; Wang, J.; Hao, X.; Xu, G.; Abudula, A.; Guan, G. Hydrogen Production from Catalytic Steam Reforming of Bio-Oils: A Critical Review. *Chem. Eng. Technol.* **2020**, *43*, 625–640. [CrossRef]
13. Zhou, W.J.; Zhou, B.; Li, W.Z.; Zhou, Z.H.; Song, S.Q.; Sun, G.Q.; Xin, Q.; Douvartzides, S.; Goula, M.; Tsiakaras, P. Performance comparison of low-temperature direct alcohol fuel cells with different anode catalysts. *J. Power Sources* **2004**, *126*, 16–22. [CrossRef]
14. Bepari, S.; Kuila, D. Steam reforming of methanol, ethanol and glycerol over nickel-based catalysts—A review. *Int. J. Hydrogen Energy* **2020**, *45*, 18090–18113. [CrossRef]
15. Ni, M.; Leung, D.Y.C.; Leung, M.K.H. A review on reforming bio-ethanol for hydrogen production. *Int. J. Hydrogen Energy* **2007**, *32*, 3238–3247. [CrossRef]
16. Liu, C.; Chen, D.; Cao, Y.; Zhang, T.; Mao, Y.; Wang, W.; Wang, Z.; Kawi, S. Catalytic steam reforming of in-situ tar from rice husk over MCM-41 supported $LaNiO_3$ to produce hydrogen rich syngas. *Renew. Energy* **2020**, *161*, 408–418. [CrossRef]
17. Zheng, B.; Shen, Y.; Sun, P.; Liu, R.; Meng, J.; Chang, R.; Gao, T.; Liu, Y. Effects of particle sizes on performances of the multi-zone steam generator using waste heat in a bio-oil steam reforming hydrogen production system. *Int. J. Hydrogen Energy* **2021**, *46*, 18064–18072. [CrossRef]
18. Garcia-Gomez, N.; Valecillos, J.; Remiro, A.; Valle, B.; Bilbao, J.; Gayubo, A.G. Effect of reaction conditions on the deactivation by coke of a $NiAl_2O_4$ spinel derived catalyst in the steam reforming of bio-oil. *Appl. Catal. B Environ.* **2021**, *297*, 120445. [CrossRef]
19. Xu, T.; Jiang, C.; Wang, X.; Xiao, B. Bio-oil chemical looping reforming coupled with water splitting for hydrogen and syngas coproduction: Effect of supports on the performance of Ni-Fe bimetallic oxygen carriers. *Energ. Convers. Manag.* **2021**, *244*, 114512. [CrossRef]
20. Siakavelas, G.I.; Charisiou, N.D.; AlKhoori, S.; AlKhoori, A.A.; Sebastian, V.; Hinder, S.J.; Baker, M.A.; Yentekakis, I.V.; Polychronopoulou, K.; Goula, M.A. Highly selective and stable nickel catalysts supported on ceria promoted with Sm_2O_3, Pr_2O_3 and MgO for the CO_2 methanation reaction. *Appl. Catal. B Environ.* **2021**, *282*, 119562. [CrossRef]
21. Global vision from the thermodynamics of the effect of the bio-oil composition and the reforming strategies in the H_2 production and the energy requirement. *Energy Convers. Manag.* **2021**, *239*, 114181. [CrossRef]
22. Kumar, A.; Chakraborty, J.P.; Singh, R. Bio-oil: The future of hydrogen generation. *Biofuels* **2017**, *8*, 663–674. [CrossRef]
23. Adeniyi, A.G.; Otoikhian, K.S.; Ighalo, J.O. Steam Reforming of Biomass Pyrolysis Oil: A Review. *Int. J. Chem. React. Eng.* **2019**, *17*, 20180328. [CrossRef]
24. Williams, C.L.; Emerson, R.M.; Tumuluru, J.S. Biomass Compositional Analysis for Conversion to Renewable Fuels and Chemicals. In *Biomass Volume Estimation and Valorization for Energy*; IntechOpen: London, UK, 2017. [CrossRef]
25. Wang, G.; Dai, Y.; Yang, H.; Xiong, Q.; Wang, K.; Zhou, J.; Li, Y.; Wang, S. A review of recent advances in biomass pyrolysis. *Energy Fuels* **2020**, *34*, 15557–15578. [CrossRef]

26. Pandey, B.; Prajapati, Y.K.; Sheth, P.N. Recent progress in thermochemical techniques to produce hydrogen gas from biomass: A state of the art review. *Int. J. Hydrogen Energy* **2019**, *44*, 25384–25415. [CrossRef]
27. Papageridis, K.N.; Charisiou, N.D.; Douvartzides, S.; Sebastian, V.; Hinder, S.J.; Baker, M.A.; AlKhoori, S.; Polychronopoulou, K.; Goula, M.A. Promoting effect of CaO-MgO mixed oxide on Ni/γ-Al_2O_3 catalyst for selective catalytic deoxygenation of palm oil. *Renew. Energy* **2020**, *162*, 1793–1810. [CrossRef]
28. Papageridis, K.N.; Charisiou, N.D.; Douvartzides, S.L.; Sebastian, V.; Hinder, S.J.; Baker, M.A.; AlKhoori, S.; Polychronopoulou, K.; Goula, M.A. Effect of operating parameters on the selective catalytic deoxygenation of palm oil to produce renewable diesel over Ni supported on Al_2O_3, ZrO_2 and SiO_2 catalysts. *Fuel Process. Technol.* **2020**, *209*, 106547. [CrossRef]
29. Charisiou, N.D.; Douvartzides, S.L.; Siakavelas, G.I.; Tzounis, L.; Sebastian, V.; Stolojan, V.; Hinder, S.J.; Baker, M.A.; Polychronopoulou, K.; Goula, M.A. The relationship between reaction temperature and carbon deposition on nickel catalysts based on Al_2O_3, ZrO_2 or SiO_2 supports during the biogas dry reforming reaction. *Catalysts* **2019**, *9*, 676. [CrossRef]
30. Martino, M.; Ruocco, C.; Meloni, E.; Pullumbi, P.; Palma, V. Main hydrogen production processes: An overview. *Catalysts* **2021**, *11*, 547. [CrossRef]
31. Abou Rjeily, M.; Gennequin, C.; Pron, H.; Abi-Aad, E.; Randrianalisoa, J.H. Pyrolysis-catalytic upgrading of bio-oil and pyrolysis-catalytic steam reforming of biogas: A review. *Environ. Chem. Lett.* **2021**, *19*, 2825–2872. [CrossRef]
32. Mohan, D.; Pittman, C.U.; Philip, S. Pyrolysis of Wood/Biomass for Bio-oil: A Critical Review. *Prog. Energy Combust. Sci.* **2017**, *62*, 848–889. [CrossRef]
33. Kejla, L.; Auersvald, M.; Šimáček, P. Combination of GC–MS and selective peak elimination procedures as a tool for characterization of complex saccharide mixtures—Application to pyrolysis bio-oils. *J. Chromatogr. B Anal. Technol. Biomed. Life Sci.* **2021**, *1171*, 122644. [CrossRef] [PubMed]
34. Branca, C.; Giudicianni, P.; Di Blasi, C. GC/MS characterization of liquids generated from low-temperature pyrolysis of wood. *Ind. Eng. Chem. Res.* **2003**, *42*, 3190–3202. [CrossRef]
35. Tahir, M.H.; Cheng, X.; Irfan, R.M.; Ashraf, R.; Zhang, Y. Comparative chemical analysis of pyrolyzed bio oil using online TGA-FTIR and GC-MS. *J. Anal. Appl. Pyrolysis* **2020**, *150*, 104890. [CrossRef]
36. Luo, Z.; Mullen, C.A.; Abdel-Haleem, H. Pyrolysis GC/MS analysis of improved guayule genotypes. *Ind. Crops Prod.* **2020**, *155*, 112810. [CrossRef]
37. Mullen, C.A.; Tarves, P.C.; Boateng, A.A. Role of Potassium Exchange in Catalytic Pyrolysis of Biomass over ZSM-5: Formation of Alkyl Phenols and Furans. *ACS Sustain. Chem. Eng.* **2017**, *5*, 2154–2162. [CrossRef]
38. Bimbela, F.; Oliva, M.; Ruiz, J.; García, L.; Arauzo, J. Catalytic steam reforming of model compounds of biomass pyrolysis liquids in fixed bed: Acetol and n-butanol. *J. Anal. Appl. Pyrolysis* **2009**, *85*, 204–213. [CrossRef]
39. Bimbela, F.; Oliva, M.; Ruiz, J.; García, L.; Arauzo, J. Hydrogen production by catalytic steam reforming of acetic acid, a model compound of biomass pyrolysis liquids. *J. Anal. Appl. Pyrolysis* **2007**, *79*, 112–120. [CrossRef]
40. Ortiz-Toral, P.J.; Satrio, J.; Brown, R.C.; Shanks, B.H. Steam reforming of bio-oil fractions: Effect of composition and stability. *Energy Fuels* **2011**, *25*, 3289–3297. [CrossRef]
41. Garcia, L.; French, R.; Czernik, S.; Chornet, E. Catalytic steam reforming of bio-oils for the production of hydrogen: Effects of catalyst composition. *Appl. Catal. A Gen.* **2000**, *201*, 225–239. [CrossRef]
42. Czernik, S.; French, R.; Feik, C.; Chornet, E. Hydrogen by Catalytic Steam Reforming of Liquid Byproducts from Biomass Thermoconversion Processes. *Ind. Eng. Chem. Res.* **2002**, *41*, 4209–4215. [CrossRef]
43. Valle, B.; Remiro, A.; Aguayo, A.T.; Bilbao, J.; Gayubo, A.G. Catalysts of Ni/α-Al_2O_3 and Ni/La_2O_3-α-Al_2O_3 for hydrogen production by steam reforming of bio-oil aqueous fraction with pyrolytic lignin retention. *Int. J. Hydrogen Energy* **2013**, *38*, 1307–1318. [CrossRef]
44. Yan, C.F.; Hu, E.Y.; Cai, C.L. Hydrogen production from bio-oil aqueous fraction with in situ carbon dioxide capture. *Int. J. Hydrogen Energy* **2010**, *35*, 2612–2616. [CrossRef]
45. Yan, C.F.; Cheng, F.F.; Hu, R.R. Hydrogen production from catalytic steam reforming of bio-oil aqueous fraction over Ni/CeO_2-ZrO_2 catalysts. *Int. J. Hydrogen Energy* **2010**, *35*, 11693–11699. [CrossRef]
46. Seyedeyn-Azad, F.; Salehi, E.; Abedi, J.; Harding, T. Biomass to hydrogen via catalytic steam reforming of bio-oil over Ni-supported alumina catalysts. *Fuel Process. Technol.* **2011**, *92*, 563–569. [CrossRef]
47. Chen, G.; Yao, J.; Liu, J.; Yan, B.; Shan, R. Biomass to hydrogen-rich syngas via catalytic steam reforming of bio-oil. *Renew. Energy* **2016**, *91*, 315–322. [CrossRef]
48. Bimbela, F.; Oliva, M.; Ruiz, J.; García, L.; Arauzo, J. Hydrogen production via catalytic steam reforming of the aqueous fraction of bio-oil using nickel-based coprecipitated catalysts. *Int. J. Hydrogen Energy* **2013**, *38*, 14476–14487. [CrossRef]
49. Valle, B.; Gayubo, A.G.; Atutxa, A.; Alonso, A.; Bilbao, J. Integration of thermal treatment and catalytic transformation for upgrading biomass pyrolysis oil. *Int. J. Chem. React. Eng.* **2007**, *5*, 86. [CrossRef]
50. Zhou, Q.; Zarei, A.; De Girolamo, A.; Yan, Y.; Zhang, L. Catalytic performance of scrap tyre char for the upgrading of eucalyptus pyrolysis derived bio-oil via cracking and deoxygenation. *J. Anal. Appl. Pyrolysis* **2019**, *139*, 167–176. [CrossRef]
51. Kumar, R.; Strezov, V. Thermochemical production of bio-oil: A review of downstream processing technologies for bio-oil upgrading, production of hydrogen and high value-added products. *Renew. Sustain. Energy Rev.* **2021**, *135*, 110152. [CrossRef]
52. Lian, X.; Xue, Y.; Zhao, Z.; Xu, G.; Han, S.; Yu, H. Progress on upgrading methods of bio-oil: A review. *Int. J. Energy Res.* **2017**, *35*, 1048–1055. [CrossRef]

53. Trane, R.; Dahl, S.; Skjøth-Rasmussen, M.S.; Jensen, A.D. Catalytic steam reforming of bio-oil. *Int. J. Hydrogen Energy* **2012**, *37*, 6447–6472. [CrossRef]
54. Arregi, A.; Amutio, M.; Lopez, G.; Bilbao, J.; Olazar, M. Evaluation of thermochemical routes for hydrogen production from biomass: A review. *Energy Convers. Manag.* **2018**, *165*, 696–719. [CrossRef]
55. Li, J.; Jia, P.; Hu, X.; Dong, D.; Gao, G.; Geng, D.; Xiang, J.; Wang, Y.; Hu, S. Steam reforming of carboxylic acids for hydrogen generation: Effects of aliphatic chain of the acids on their reaction behaviors. *Mol. Catal.* **2018**, *450*, 1–13. [CrossRef]
56. Li, J.; Mei, X.; Zhang, L.; Yu, Z.; Liu, Q.; Wei, T.; Wu, W.; Dong, D.; Xu, L.; Hu, X. A comparative study of catalytic behaviors of Mn, Fe, Co, Ni, Cu and Zn–Based catalysts in steam reforming of methanol, acetic acid and acetone. *Int. J. Hydrogen Energy* **2020**, *45*, 3815–3832. [CrossRef]
57. Li, D.; Xue, H.; Hu, R. Effect of Ce/Ca Ratio in Ni/CeO_2-ZrO_2-CaO Catalysts on High-Purity Hydrogen Production by Sorption-Enhanced Steam Reforming of Acetic Acid and Bio-Oil. *Ind. Eng. Chem. Res.* **2020**, *59*, 1446–1456. [CrossRef]
58. Zhang, L.; Yu, Z.; Li, J.; Zhang, S.; Hu, S.; Xiang, J.; Wang, Y.; Liu, Q.; Hu, G.; Hu, X. Steam reforming of typical small organics derived from bio-oil: Correlation of their reaction behaviors with molecular structures. *Fuel* **2020**, *259*, 116214. [CrossRef]
59. Zheng, X.X.; Yan, C.F.; Hu, R.R.; Li, J.; Hai, H.; Luo, W.M.; Guo, C.Q.; Li, W.B.; Zhou, Z.Y. Hydrogen from acetic acid as the model compound of biomass fast-pyralysis oil over Ni catalyst supported on ceria-zirconia. *Int. J. Hydrogen Energy* **2012**, *37*, 12987–12993. [CrossRef]
60. Hu, X.; Lu, G. Investigation of steam reforming of acetic acid to hydrogen over Ni-Co metal catalyst. *J. Mol. Catal. A Chem.* **2007**, *261*, 43–48. [CrossRef]
61. Liu, C.; Li, S.; Chen, D.; Xiao, Y.; Li, T.; Wang, W. Hydrogen-rich syngas production by chemical looping steam reforming of acetic acid as bio-oil model compound over Fe-doped $LaNiO_3$ oxygen carriers. *Int. J. Hydrogen Energy* **2019**, *44*, 17732–17741. [CrossRef]
62. Liu, C.L.; Chen, D.; Wang, W. Hydrogen-rich syngas production from chemical looping steam reforming of bio-oil model compound: Effect of bimetal on $LaNi_{0.8}M_{0.2}O_3$ (M = Fe, Co, Cu, and Mn). *Int. J. Energy Res.* **2019**, *43*, 4534–4545. [CrossRef]
63. Vagia, E.C.; Lemonidou, A.A. Hydrogen production via steam reforming of bio-oil components over calcium aluminate supported nickel and noble metal catalysts. *Appl. Catal. A Gen.* **2008**, *351*, 111–121. [CrossRef]
64. Vagia, E.C.; Lemonidou, A.A. Investigations on the properties of ceria-zirconia-supported Ni and Rh catalysts and their performance in acetic acid steam reforming. *J. Catal.* **2010**, *269*, 388–396. [CrossRef]
65. Megía, P.J.; Carrero, A.; Calles, J.A.; Vizcaíno, A.J. Hydrogen production from steam reforming of acetic acid as a model compound of the aqueous fraction of microalgae HTL using Co-M/SBA-15 (M: Cu, Ag, Ce, Cr) catalysts. *Catalysts* **2019**, *9*, 1013. [CrossRef]
66. Megía, P.J.; Calles, J.A.; Carrero, A.; Vizcaíno, A.J. Effect of the incorporation of reducibility promoters (Cu, Ce, Ag) in Co/CaSBA-15 catalysts for acetic acid steam reforming. *Int. J. Energy Res.* **2021**, *45*, 1685–1702. [CrossRef]
67. Resende, K.A.; Ávila-Neto, C.N.; Rabelo-Neto, R.C.; Noronha, F.B.; Hori, C.E. Hydrogen production by reforming of acetic acid using La-Ni type perovskites partially substituted with Sm and Pr. *Catal. Today* **2015**, *242*, 71–79. [CrossRef]
68. Takanabe, K.; Aika, K.I.; Seshan, K.; Lefferts, L. Sustainable hydrogen from bio-oil—Steam reforming of acetic acid as a model oxygenate. *J. Catal.* **2004**, *227*, 101–108. [CrossRef]
69. Takanabe, K.; Aika, K.i.; Seshan, K.; Lefferts, L. Catalyst deactivation during steam reforming of acetic acid over Pt/ZrO_2. *Chem. Eng. J.* **2006**, *120*, 133–137. [CrossRef]
70. Rioche, C.; Kulkarni, S.; Meunier, F.C.; Breen, J.P.; Burch, R. Steam reforming of model compounds and fast pyrolysis bio-oil on supported noble metal catalysts. *Appl. Catal. B Environ.* **2005**, *61*, 130–139. [CrossRef]
71. Li, L.; Jiang, B.; Tang, D.; Zhang, Q.; Zheng, Z. Hydrogen generation by acetic acid steam reforming over Ni-based catalysts derived from $La_{1-x}Ce_xNiO_3$ perovskite. *Int. J. Hydrogen Energy* **2018**, *43*, 6795–6803. [CrossRef]
72. Wang, D.; Czernik, S.; Montané, D.; Mann, M.; Chornet, E. Biomass to Hydrogen via Fast Pyrolysis and Catalytic Steam Reforming of the Pyrolysis Oil or Its Fractions. *Ind. Eng. Chem. Res.* **1997**, *36*, 1507–1518. [CrossRef]
73. Wang, S.; Li, X.; Guo, L.; Luo, Z. Experimental research on acetic acid steam reforming over Co-Fe catalysts and subsequent density functional theory studies. *Int. J. Hydrogen Energy* **2012**, *37*, 11122–11131. [CrossRef]
74. Wang, S.; Cai, Q.; Zhang, F.; Li, X.; Zhang, L.; Luo, Z. Hydrogen production via catalytic reforming of the bio-oil model compounds: Acetic acid, phenol and hydroxyacetone. *Int. J. Hydrogen Energy* **2014**, *39*, 18675–18687. [CrossRef]
75. Wang, Y.; Chen, M.; Liang, T.; Yang, Z.; Yang, J.; Liu, S. Hydrogen generation from catalytic steam reforming of acetic acid by Ni/attapulgite catalysts. *Catalysts* **2016**, *6*, 172. [CrossRef]
76. Assaf, P.G.M.; Nogueira, F.G.E.; Assaf, E.M. Ni and Co catalysts supported on alumina applied to steam reforming of acetic acid: Representative compound for the aqueous phase of bio-oil derived from biomass. *Catal. Today* **2013**, *213*, 2–8. [CrossRef]
77. Hu, X.; Zhang, L.; Lu, G. Pruning of the surface species on Ni/Al_2O_3 catalyst to selective production of hydrogen via acetone and acetic acid steam reforming. *Appl. Catal. A Gen.* **2012**, *427–428*, 49–57. [CrossRef]
78. Pant, K.K.; Mohanty, P.; Agarwal, S.; Dalai, A.K. Steam reforming of acetic acid for hydrogen production over bifunctional Ni-Co catalysts. *Catal. Today* **2013**, *207*, 36–43. [CrossRef]
79. Cheng, F.; Dupont, V. Nickel catalyst auto-reduction during steam reforming of bio-oil model compound acetic acid. *Int. J. Hydrogen Energy* **2013**, *38*, 15160–15172. [CrossRef]
80. Choi, I.H.; Hwang, K.R.; Lee, K.Y.; Lee, I.G. Catalytic steam reforming of biomass-derived acetic acid over modified Ni/Γ-Al_2O_3 for sustainable hydrogen production. *Int. J. Hydrogen Energy* **2019**, *44*, 180–190. [CrossRef]

81. Basagiannis, A.C.; Verykios, X.E. Catalytic steam reforming of acetic acid for hydrogen production. *Int. J. Hydrogen Energy* **2007**, *32*, 3343–3355. [CrossRef]
82. Junior, R.B.S.; Rabelo-Neto, R.C.; Gomes, R.S.; Noronha, F.B.; Fréty, R.; Brandão, S.T. Steam reforming of acetic acid over Ni-based catalysts derived from $La_{1-x}Ca_xNiO_3$ perovskite type oxides. *Fuel* **2019**, *254*, 115714. [CrossRef]
83. Montero, C.; Oar-Arteta, L.; Remiro, A.; Arandia, A.; Bilbao, J.; Gayubo, A.G. Thermodynamic comparison between bio-oil and ethanol steam reforming. *Int. J. Hydrogen Energy* **2015**, *40*, 15963–15971. [CrossRef]
84. Vizcaíno, A.J.; Carrero, A.; Calles, J.A. Comparison of ethanol steam reforming using Co and Ni catalysts supported on SBA-15 modified by Ca and Mg. *Fuel Process. Technol.* **2016**, *146*, 99–109. [CrossRef]
85. Alberton, A.L.; Souza, M.M.V.M.; Schmal, M. Carbon formation and its influence on ethanol steam reforming over Ni/Al_2O_3 catalysts. *Catal. Today* **2007**, *123*, 257–264. [CrossRef]
86. Goula, M.A.; Kontou, S.K.; Tsiakaras, P.E. Hydrogen production by ethanol steam reforming over a commercial $Pd/\gamma\text{-}Al_2O_3$ catalyst. *Appl. Catal. B Environ.* **2004**, *49*, 135–144. [CrossRef]
87. Montero, C.; Remiro, A.; Arandia, A.; Benito, P.L.; Bilbao, J.; Gayubo, A.G. Reproducible performance of a $Ni/La_2O_3\text{–}\alpha Al_2O_3$ catalyst in ethanol steam reforming under reaction–regeneration cycles. *Fuel Process. Technol.* **2016**, *152*, 215–222. [CrossRef]
88. Profeti, L.P.R.; Dias, J.A.C.; Assaf, J.M.; Assaf, E.M. Hydrogen production by steam reforming of ethanol over Ni-based catalysts promoted with noble metals. *J. Power Sources* **2009**, *190*, 525–533. [CrossRef]
89. Italiano, C.; Bizkarra, K.; Barrio, V.L.; Cambra, J.F.; Pino, L.; Vita, A. Renewable hydrogen production via steam reforming of simulated bio-oil over Ni-based catalysts. *Int. J. Hydrogen Energy* **2019**, *44*, 14671–14682. [CrossRef]
90. Bizkarra, K.; Barrio, V.L.; Gartzia-Rivero, L.; Bañuelos, J.; López-Arbeloa, I.; Cambra, J.F. Hydrogen production from a model bio-oil/bio-glycerol mixture through steam reforming using Zeolite L supported catalysts. *Int. J. Hydrogen Energy* **2019**, *44*, 1492–1504. [CrossRef]
91. Papageridis, K.N.; Siakavelas, G.; Charisiou, N.D.; Avraam, D.G.; Tzounis, L.; Kousi, K.; Goula, M.A. Comparative study of Ni, Co, Cu supported on γ-alumina catalysts for hydrogen production via the glycerol steam reforming reaction. *Fuel Process. Technol.* **2016**, *152*, 156–175. [CrossRef]
92. Charisiou, N.D.; Italiano, C.; Pino, L.; Sebastian, V.; Vita, A.; Goula, M.A. Hydrogen production via steam reforming of glycerol over $Rh/\gamma\text{-}Al_2O_3$ catalysts modified with CeO_2, MgO or La_2O_3. *Renew. Energy* **2020**, *162*, 908–925. [CrossRef]
93. Polychronopoulou, K.; Charisiou, N.D.; Siakavelas, G.I.; Alkhoori, A.A.; Sebastian, V.; Hinder, S.J.; Baker, M.A.; Goula, M.A. Ce-Sm-x Cu cost-efficient catalysts for H_2 production through the glycerol steam reforming reaction. *Sustain. Energy Fuels* **2019**, *3*, 673–691. [CrossRef]
94. Polychronopoulou, K.; Charisiou, N.; Papageridis, K.; Sebastian, V.; Hinder, S.; Dabbawala, A.; Alkhoori, A.; Baker, M.; Goula, M. The effect of Ni addition onto a Cu-based ternary support on the H_2 production over glycerol steam reforming reaction. *Nanomaterials* **2018**, *8*, 931. [CrossRef]
95. Takanabe, K.; Aika, K.I.; Inazu, K.; Baba, T.; Seshan, K.; Lefferts, L. Steam reforming of acetic acid as a biomass derived oxygenate: Bifunctional pathway for hydrogen formation over Pt/ZrO_2 catalysts. *J. Catal.* **2006**, *243*, 263–269. [CrossRef]
96. Braga, A.H.; Sodré, E.R.; Santos, J.B.O.; de Paula Marques, C.M.; Bueno, J.M.C. Steam reforming of acetone over Ni- and Co-based catalysts: Effect of the composition of reactants and catalysts on reaction pathways. *Appl. Catal. B Environ.* **2016**, *195*, 16–28. [CrossRef]
97. Navarro, R.M.; Guil-Lopez, R.; Gonzalez-Carballo, J.M.; Cubero, A.; Ismail, A.A.; Al-Sayari, S.A.; Fierro, J.L.G. Bimetallic MNi/Al_2O_3-La catalysts (M = Pt, Cu) for acetone steam reforming: Role of M on catalyst structure and activity. *Appl. Catal. A Gen.* **2014**, *474*, 168–177. [CrossRef]
98. Polychronopoulou, K.; Bakandritsos, A.; Tzitzios, V.; Fierro, J.L.G.; Efstathiou, A.M. Absorption-enhanced reforming of phenol by steam over supported Fe catalysts. *J. Catal.* **2006**, *241*, 132–148. [CrossRef]
99. Ramos, M.C.; Navascués, A.I.; García, L. Rafael Bilbao Hydrogen Production by Catalytic Steam Reforming of Acetol, a Model Compound of Bio-Oil. *Ind. Eng. Chem. Res.* **2007**, *46*, 2399–2406. [CrossRef]
100. García-Gómez, N.; Valle, B.; Valecillos, J.; Remiro, A.; Bilbao, J.; Gayubo, A.G. Feasibility of online pre-reforming step with dolomite for improving Ni spinel catalyst stability in the steam reforming of raw bio-oil. *Fuel Process. Technol.* **2021**, *215*, 106769. [CrossRef]
101. Setiabudi, H.D.; Aziz, M.A.A.; Abdullah, S.; Teh, L.P.; Jusoh, R. Hydrogen production from catalytic steam reforming of biomass pyrolysis oil or bio-oil derivatives: A review. *Int. J. Hydrogen Energy* **2020**, *45*, 18376–18397. [CrossRef]
102. Ayalur Chattanathan, S.; Adhikari, S.; Abdoulmoumine, N. A review on current status of hydrogen production from bio-oil. *Renew. Sustain. Energy Rev.* **2012**, *16*, 2366–2372. [CrossRef]
103. Baviskar, C.V.; Vaidya, P.D. Steam reforming of model bio-oil compounds 2-butanone, 1-methoxy-2-propanol, ethyl acetate and butyraldehyde over Ni/Al_2O_3. *Int. J. Hydrogen Energy* **2017**, *42*, 21667–21676. [CrossRef]
104. Zhang, L.; Hu, X.; Hu, K.; Hu, C.; Zhang, Z.; Liu, Q.; Hu, S.; Xiang, J.; Wang, Y.; Zhang, S. Progress in the reforming of bio-oil derived carboxylic acids for hydrogen generation. *J. Power Sources* **2018**, *403*, 137–156. [CrossRef]
105. Hu, X.; Zhang, Z.; Gholizadeh, M.; Zhang, S.; Lam, C.H.; Xiong, Z.; Wang, Y.; Rostrup-Nielsen, J.R. Coke formation during thermal treatment of bio-oil. *Energy Fuels* **2020**, *34*, 225–232. [CrossRef]
106. Kumar, A.; Singh, R.; Sinha, A.S.K. Catalyst modification strategies to enhance the catalyst activity and stability during steam reforming of acetic acid for hydrogen production. *Int. J. Hydrogen Energy* **2019**, *44*, 12983–13010. [CrossRef]

107. Nabgan, W.; Tuan Abdullah, T.A.; Mat, R.; Nabgan, B.; Gambo, Y.; Ibrahim, M.; Ahmad, A.; Jalil, A.A.; Triwahyono, S.; Saeh, I. Renewable hydrogen production from bio-oil derivative via catalytic steam reforming: An overview. *Renew. Sustain. Energy Rev.* **2017**, *79*, 347–357. [CrossRef]
108. Wang, D.; Czernik, S.; Chornet, E. Production of hydrogen from biomass by catalytic steam reforming of fast pyrolysis oils. *Energy Fuels* **1998**, *12*, 19–24. [CrossRef]
109. Basagiannis, A.C.; Verykios, X.E. Steam reforming of the aqueous fraction of bio-oil over structured Ru/MgO/Al_2O_3 catalysts. *Catal. Today* **2007**, *127*, 256–264. [CrossRef]
110. Kechagiopoulos, P.N.; Voutetakis, S.S.; Lemonidou, A.A.; Vasalos, I.A. Sustainable hydrogen production via reforming of ethylene glycol using a novel spouted bed reactor. *Catal. Today* **2007**, *127*, 246–255. [CrossRef]
111. Kechagiopoulos, P.N.; Voutetakis, S.S.; Lemonidou, A.A.; Vasalos, I.A. Hydrogen production via reforming of the aqueous phase of bio-oil over Ni/olivine catalysts in a spouted bed reactor. *Ind. Eng. Chem. Res.* **2009**, *48*, 1400–1408. [CrossRef]
112. Vagia, E.C.; Lemonidou, A.A. Thermodynamic analysis of hydrogen production via steam reforming of selected components of aqueous bio-oil fraction. *Int. J. Hydrogen Energy* **2007**, *32*, 212–223. [CrossRef]
113. Vagia, E.C.; Lemonidou, A.A. Thermodynamic analysis of hydrogen production via autothermal steam reforming of selected components of aqueous bio-oil fraction. *Int. J. Hydrogen Energy* **2008**, *33*, 2489–2500. [CrossRef]
114. Wu, C.; Liu, R. Carbon deposition behavior in steam reforming of bio-oil model compound for hydrogen production. *Int. J. Hydrogen Energy* **2010**, *35*, 7386–7398. [CrossRef]
115. Guan, G.; Kaewpanha, M.; Hao, X.; Abudula, A. Catalytic steam reforming of biomass tar: Prospects and challenges. *Renew. Sustain. Energy Rev.* **2016**, *58*, 450–461. [CrossRef]
116. Charisiou, N.D.; Siakavelas, G.I.; Dou, B.; Sebastian, V.; Hinder, S.J.; Baker, M.A.; Polychronopoulou, K.; Goula, M.A. Nickel supported on $AlCeO_3$ as a highly selective and stable catalyst for hydrogen production via the glycerol steam reforming reaction. *Catalysts* **2019**, *9*, 411. [CrossRef]
117. Jeong, C.M.; Park, G.W.; Choi, J.D.R.; Kang, J.W.; Kim, S.M.; Lee, W.H.; Woo, S.I.; Chang, H.N. Steam reforming of volatile fatty acids (VFAs) over supported Pt/Al_2O_3 catalysts. *Int. J. Hydrogen Energy* **2011**, *36*, 7505–7515. [CrossRef]
118. Charisiou, N.D.; Sebastian, V.; Hinder, S.J.; Baker, M.A.; Polychronopoulou, K.; Goula, M.A. Ni catalysts based on attapulgite for hydrogen production through the glycerol steam reforming reaction. *Catalysts* **2019**, *9*, 650–669. [CrossRef]
119. Wang, D.; Montané, D.; Chornet, E. Catalytic steam reforming of biomass-derived oxygenates: Acetic acid and hydroxyacetaldehyde. *Appl. Catal. A Gen.* **1996**, *143*, 245–270. [CrossRef]
120. Czernik, S.; Evans, R.; French, R. Hydrogen from biomass-production by steam reforming of biomass pyrolysis oil. *Catal. Today* **2007**, *129*, 265–268. [CrossRef]
121. Goyal, N.; Pant, K.K.; Gupta, R. Hydrogen production by steam reforming of model bio-oil using structured Ni/Al_2O_3 catalysts. *Int. J. Hydrogen Energy* **2013**, *38*, 921–933. [CrossRef]
122. Tsiotsias, A.I.; Charisiou, N.D.; Yentekakis, I.V.; Goula, M.A. The role of alkali and alkaline earth metals in the CO_2 methanation reaction and the combined capture and methanation of CO_2. *Catalysts* **2020**, *10*, 812. [CrossRef]
123. Davidian, T.; Guilhaume, N.; Iojoiu, E.; Provendier, H.; Mirodatos, C. Hydrogen production from crude pyrolysis oil by a sequential catalytic process. *Appl. Catal. B Environ.* **2007**, *73*, 116–127. [CrossRef]
124. Lan, P.; Xu, Q.; Zhou, M.; Lan, L.; Zhang, S.; Yan, Y. Catalytic steam reforming of fast pyrolysis bio-oil in fixed bed and fluidized bed reactors. *Chem. Eng. Technol.* **2010**, *33*, 2021–2028. [CrossRef]
125. Wang, S.; Zhang, F.; Cai, Q.; Li, X.; Zhu, L.; Wang, Q.; Luo, Z. Catalytic steam reforming of bio-oil model compounds for hydrogen production over coal ash supported Ni catalyst. *Int. J. Hydrogen Energy* **2014**, *39*, 2018–2025. [CrossRef]
126. Román Galdámez, J.; García, L.; Bilbao, R. Hydrogen production by steam reforming of bio-oil using coprecipitated Ni-Al catalysts. Acetic acid as a model compound. *Energy Fuels* **2005**, *19*, 1133–1142. [CrossRef]
127. Nogueira, F.G.E.; Assaf, P.G.M.; Carvalho, H.W.P.; Assaf, E.M. Catalytic steam reforming of acetic acid as a model compound of bio-oil. *Appl. Catal. B Environ.* **2014**, *160–161*, 188–199. [CrossRef]
128. Yao, D.; Wu, C.; Yang, H.; Hu, Q.; Nahil, M.A.; Chen, H.; Williams, P.T. Hydrogen production from catalytic reforming of the aqueous fraction of pyrolysis bio-oil with modified Ni-Al catalysts. *Int. J. Hydrogen Energy* **2014**, *39*, 14642–14652. [CrossRef]
129. Chen, J.; Sun, J.; Wang, Y. Catalysts for Steam Reforming of Bio-oil: A Review. *Ind. Eng. Chem. Res.* **2017**, *56*, 4627–4637. [CrossRef]
130. Lemonidou, A.A.; Kechagiopoulos, P.; Heracleous, E.; Voutetakis, S. Steam Reforming of Bio-oils to Hydrogen. In *The Role of Catalysis for the Sustainable Production of Bio-Fuels and Bio-Chemicals*; Elsevier: Amsterdam, The Netherlands, 2013; pp. 467–493. [CrossRef]
131. Chaudhary, V.; Sharma, S. An overview of ordered mesoporous material SBA-15: Synthesis, functionalization and application in oxidation reactions. *J. Porous Mater.* **2017**, *24*, 741–749. [CrossRef]
132. Garcia-Garcia, I.; Acha, E.; Bizkarra, K.; Martinez De Ilarduya, J.; Requies, J.; Cambra, J.F. Hydrogen production by steam reforming of m-cresol, a bio-oil model compound, using catalysts supported on conventional and unconventional supports. *Int. J. Hydrogen Energy* **2015**, *40*, 14445–14455. [CrossRef]
133. Seyedeyn Azad, F.; Abedi, J.; Salehi, E.; Harding, T. Production of hydrogen via steam reforming of bio-oil over Ni-based catalysts: Effect of support. *Chem. Eng. J.* **2012**, *180*, 145–150. [CrossRef]
134. Salehi, E.; Azad, F.S.; Harding, T.; Abedi, J. Production of hydrogen by steam reforming of bio-oil over Ni/Al_2O_3 catalysts: Effect of addition of promoter and preparation procedure. *Fuel Process. Technol.* **2011**, *92*, 2203–2210. [CrossRef]

135. Llorca, J.; Homs, N.; Sales, J.; Ramírez de la Piscina, P. Efficient production of hydrogen over supported cobalt catalysts from ethanol steam reforming. *J. Catal.* **2002**, *209*, 306–317. [CrossRef]
136. Mohanty, P.; Patel, M.; Pant, K.K. Hydrogen production from steam reforming of acetic acid over Cu-Zn supported calcium aluminate. *Bioresour. Technol.* **2012**, *123*, 558–565. [CrossRef] [PubMed]
137. Khzouz, M.; Wood, J.; Pollet, B.; Bujalski, W. Characterization and activity test of commercial Ni/Al_2O_3, $Cu/ZnO/Al_2O_3$ and prepared $Ni\text{-}Cu/Al_2O_3$ catalysts for hydrogen production from methane and methanol fuels. *Int. J. Hydrogen Energy* **2013**, *38*, 1664–1675. [CrossRef]
138. Pekmezci Karaman, B.; Cakiryilmaz, N.; Arbag, H.; Oktar, N.; Dogu, G.; Dogu, T. Performance comparison of mesoporous alumina supported Cu & Ni based catalysts in acetic acid reforming. *Int. J. Hydrogen Energy* **2017**, *42*, 26257–26269. [CrossRef]
139. Liu, C.; Chen, D.; Ashok, J.; Hongmanorom, P.; Wang, W.; Li, T.; Wang, Z.; Kawi, S. Chemical looping steam reforming of bio-oil for hydrogen-rich syngas production: Effect of doping on $LaNi_{0.8}Fe_{0.2}O_3$ perovskite. *Int. J. Hydrogen Energy* **2020**, *45*, 21123–21137. [CrossRef]
140. Goula, M.A.; Charisiou, N.D.; Papageridis, K.N.; Siakavelas, G. Influence of the synthesis method parameters used to prepare nickel-based catalysts on the catalytic performance for the glycerol steam reforming reaction. *Cuihua Xuebao/Chin. J. Catal.* **2016**, *37*, 1949–1965. [CrossRef]
141. Nabgan, W.; Abdullah, T.A.T.; Mat, R.; Nabgan, B.; Jalil, A.A.; Firmansyah, L.; Triwahyono, S. Production of hydrogen via steam reforming of acetic acid over Ni and Co supported on La_2O_3 catalyst. *Int. J. Hydrogen Energy* **2017**, *42*, 8975–8985. [CrossRef]
142. Valle, B.; Aramburu, B.; Benito, P.L.; Bilbao, J.; Gayubo, A.G. Biomass to hydrogen-rich gas via steam reforming of raw bio-oil over $Ni/La_2O_3\text{-}\alpha Al_2O_3$ catalyst: Effect of space-time and steam-to-carbon ratio. *Fuel* **2018**, *216*, 445–455. [CrossRef]
143. Zhang, F.; Wang, N.; Yang, L.; Li, M.; Huang, L. Ni-Co bimetallic MgO-based catalysts for hydrogen production via steam reforming of acetic acid from bio-oil. *Int. J. Hydrogen Energy* **2014**, *39*, 18688–18694. [CrossRef]
144. Gao, N.; Han, Y.; Quan, C.; Wu, C. Promoting hydrogen-rich syngas production from catalytic reforming of biomass pyrolysis oil on nanosized nickel-ceramic catalysts. *Appl. Therm. Eng.* **2017**, *125*, 297–305. [CrossRef]
145. Sehested, J. Four challenges for nickel steam-reforming catalysts. *Catal. Today* **2006**, *111*, 103–110. [CrossRef]
146. Ochoa, A.; Valle, B.; Resasco, D.E.; Bilbao, J.; Gayubo, A.G.; Castaño, P. Temperature Programmed Oxidation Coupled with In Situ Techniques Reveal the Nature and Location of Coke Deposited on a $Ni/La_2O_3\text{-}\alpha Al_2O_3$ Catalyst in the Steam Reforming of Bio-oil. *ChemCatChem* **2018**, *10*, 2311–2321. [CrossRef]
147. Valle, B.; Aramburu, B.; Olazar, M.; Bilbao, J.; Gayubo, A.G. Steam reforming of raw bio-oil over $Ni/La_2O_3\text{-}aAl_2O_3$: Influence of temperature on product yields and catalyst deactivation. *Fuel* **2018**, *216*, 463–474. [CrossRef]
148. Charisiou, N.D.; Tzounis, L.; Sebastian, V.; Hinder, S.J.; Baker, M.A.; Polychronopoulou, K.; Goula, M.A. Investigating the correlation between deactivation and the carbon deposited on the surface of Ni/Al_2O_3 and $Ni/La_2O3\text{-}Al_2O_3$ catalysts during the biogas reforming reaction. *Appl. Surf. Sci.* **2019**, *474*, 42–56. [CrossRef]
149. Charisiou, N.D.; Siakavelas, G.; Tzounis, L.; Sebastian, V.; Monzon, A.; Baker, M.A.; Hinder, S.J.; Polychronopoulou, K.; Yentekakis, I.V.; Goula, M.A. An in depth investigation of deactivation through carbon formation during the biogas dry reforming reaction for Ni supported on modified with CeO_2 and La_2O_3 zirconia catalysts. *Int. J. Hydrogen Energy* **2018**, *43*, 18955–18976. [CrossRef]
150. Chen, G.; Tao, J.; Liu, C.; Yan, B.; Li, W.; Li, X. Hydrogen production via acetic acid steam reforming: A critical review on catalysts. *Renew. Sustain. Energy Rev.* **2017**, *79*, 1091–1098. [CrossRef]
151. Beatriz, V.; Garcı´a-Gomez, N.; Arandia, A.; Remiro, A.; Bilbao, J.; Gayubo, A.G. Effect of phenols extraction on the behavior of Ni-spinel derived catalyst for raw bio-oil steam reforming. *Int. J. Hydrogen Energy* **2019**, *44*, 12593–12603.
152. Trimm, D.L. Coke formation and minimisation during steam reforming reactions. *Catal. Today* **1997**, *37*, 233–238. [CrossRef]
153. Rostrup-Nielsen, J.R. Industrial relevance of coking. *Catal. Today* **1997**, *37*, 225–232. [CrossRef]
154. Remiro, A.; Valle, B.; Aguayo, A.T.; Bilbao, J.; Gayubo, A.G. Operating conditions for attenuating $Ni/La_2O_3\text{-}\alpha Al_2O_3$ catalyst deactivation in the steam reforming of bio-oil aqueous fraction. *Fuel Process. Technol.* **2013**, *115*, 222–232. [CrossRef]
155. Sehested, J.; Larsen, N.W.; Falsig, H.; Hinnemann, B. Sintering of nickel steam reforming catalysts: Effective mass diffusion constant for Ni-OH at nickel surfaces. *Catal. Today* **2014**, *228*, 22–31. [CrossRef]
156. Sehested, J.; Gelten, J.A.P.; Helveg, S. Sintering of nickel catalysts: Effects of time, atmosphere, temperature, nickel-carrier interactions, and dopants. *Appl. Catal. A Gen.* **2006**, *309*, 237–246. [CrossRef]
157. Sehested, J. Sintering of nickel steam-reforming catalysts. *J. Catal.* **2003**, *217*, 417–426. [CrossRef]
158. Sehested, J.; Carlsson, A.; Janssens, T.V.W.; Hansen, P.L.; Datyey, A.K. Sintering of nickel steam-reforming catalysts on $MgAl_2O_4$ spinel supports. *J. Catal.* **2001**, *197*, 200–209. [CrossRef]
159. Sehested, J.; Gelten, J.A.P.; Remediakis, I.N.; Bengaard, H.; Nørskov, J.K. Sintering of nickel steam-reforming catalysts: Effects of temperature and steam and hydrogen pressures. *J. Catal.* **2004**, *223*, 432–443. [CrossRef]
160. Cui, Y.; Galvita, V.; Rihko-Struckmann, L.; Lorenz, H.; Sundmacher, K. Steam reforming of glycerol: The experimental activity of $La_{1\text{-}x}Ce_xNiO_3$ catalyst in comparison to the thermodynamic reaction equilibrium. *Appl. Catal. B Environ.* **2009**, *90*, 29–37. [CrossRef]
161. Li, Z.; Hu, X.; Zhang, L.; Liu, S.; Lu, G. Steam reforming of acetic acid over Ni/ZrO_2 catalysts: Effects of nickel loading and particle size on product distribution and coke formation. *Appl. Catal. A Gen.* **2012**, *417–418*, 281–289. [CrossRef]

162. Zhao, X.; Xue, Y.; Yan, C.; Huang, Y.; Lu, Z.; Wang, Z.; Zhang, L.; Guo, C. Promoted activity of porous silica coated Ni/CeO_2–ZrO_2 catalyst for steam reforming of acetic acid. *Int. J. Hydrogen Energy* **2017**, *42*, 21677–21685. [CrossRef]
163. Pu, J.; Nishikado, K.; Wang, N.; Nguyen, T.T.; Maki, T.; Qian, E.W. Core-shell nickel catalysts for the steam reforming of acetic acid. *Appl. Catal. B Environ.* **2018**, *224*, 69–79. [CrossRef]
164. Hu, X.; Lu, G. Comparative study of alumina-supported transition metal catalysts for hydrogen generation by steam reforming of acetic acid. *Appl. Catal. B Environ.* **2010**, *99*, 289–297. [CrossRef]
165. Azad, A.M.; Duran, M.J.; McCoy, A.K.; Abraham, M.A. Development of ceria-supported sulfur tolerant nanocatalysts: Pd-based formulations. *Appl. Catal. A Gen.* **2007**, *332*, 225–236. [CrossRef]
166. Sato, K.; Fujimoto, K. Development of new nickel based catalyst for tar reforming with superior resistance to sulfur poisoning and coking in biomass gasification. *Catal. Commun.* **2007**, *8*, 1697–1701. [CrossRef]
167. Lu, Y.; Chen, J.; Liu, Y.; Xue, Q.; He, M. Highly sulfur-tolerant Pt/$Ce_{0.8}Gd_{0.2}O_{1.9}$ catalyst for steam reforming of liquid hydrocarbons in fuel cell applications. *J. Catal.* **2008**, *254*, 39–48. [CrossRef]
168. Rostrup-Nielsen, J.R.; Sehested, J.; Nørskov, J.K. Hydrogen and synthesis gas by steam- and CO_2 reforming. *Adv. Catal.* **2002**, *47*, 65–139. [CrossRef]
169. Rostrup-Nielsen, J.R. Sulfur-passivated nickel catalysts for carbon-free steam reforming of methane. *J. Catal.* **1984**, *85*, 31–43. [CrossRef]
170. Georgiadis, A.G.; Charisiou, N.D.; Goula, M.A. Removal of hydrogen sulfide from various industrial gases: A review of the most promising adsorbing materials. *Catalysts* **2020**, *10*, 521. [CrossRef]
171. Georgiadis, A.G.; Charisiou, N.; Yentekakis, I.V.; Goula, M.A. Hydrogen sulfide (H_2S) Removal via MOFs. *Materials* **2020**, *13*, 3640. [CrossRef] [PubMed]
172. Georgiadis, A.G.; Charisiou, N.D.; Gaber, S.; Polychronopoulou, K.; Yentekakis, I.V.; Goula, M.A. Adsorption of Hydrogen Sulfide at Low Temperatures Using an Industrial Molecular Sieve: An Experimental and Theoretical Study. *ACS Omega* **2021**, *6*, 14774–14787. [CrossRef] [PubMed]
173. Wu, C.; Liu, R. Sustainable hydrogen production from steam reforming of bio-oil model compound based on carbon deposition/elimination. *Int. J. Hydrogen Energy* **2011**, *36*, 2860–2868. [CrossRef]
174. Oar-Arteta, L.; Remiro, A.; Vicente, J.; Aguayo, A.T.; Bilbao, J.; Gayubo, A.G. Stability of $CuZnOAl_2O_3$/HZSM-5 and $CuFe_2O_4$/HZSM-5 catalysts in dimethyl ether steam reforming operating in reaction-regeneration cycles. *Fuel Process. Technol.* **2014**, *126*, 145–154. [CrossRef]
175. Wang, Z.; Pan, Y.; Dong, T.; Zhu, X.; Kan, T.; Yuan, L.; Torimoto, Y.; Sadakata, M.; Li, Q. Production of hydrogen from catalytic steam reforming of bio-oil using C12A7-O^--based catalysts. *Appl. Catal. A Gen.* **2007**, *320*, 24–34. [CrossRef]
176. Arregi, A.; Barbarias, I.; Alvarez, J.; Erkiaga, A.; Artetxe, M.; Amutio, M.; Olazar, M. Hydrogen production from biomass pyrolysis and in-line catalytic steam reforming. *Chem. Eng. Trans.* **2015**, *43*, 547–552. [CrossRef]
177. Arregi, A.; Amutio, M.; Lopez, G.; Artetxe, M.; Alvarez, J.; Bilbao, J.; Olazar, M. Hydrogen-rich gas production by continuous pyrolysis and in-line catalytic reforming of pine wood waste and HDPE mixtures. *Energy Convers. Manag.* **2017**, *136*, 192–201. [CrossRef]
178. Arregi, A.; Lopez, G.; Amutio, M.; Artetxe, M.; Barbarias, I.; Bilbao, J.; Olazar, M. Role of operating conditions in the catalyst deactivation in the in-line steam reforming of volatiles from biomass fast pyrolysis. *Fuel* **2018**, *216*, 233–244. [CrossRef]
179. Ma, Z.; Zhang, S.P.; Xie, D.Y.; Yan, Y.J. A novel integrated process for hydrogen production from biomass. *Int. J. Hydrogen Energy* **2014**, *39*, 1274–1279. [CrossRef]
180. Chen, F.; Wu, C.; Dong, L.; Vassallo, A.; Williams, P.T.; Huang, J. Characteristics and catalytic properties of Ni/$CaAlO_x$ catalyst for hydrogen-enriched syngas production from pyrolysis-steam reforming of biomass sawdust. *Appl. Catal. B Environ.* **2016**, *183*, 168–175. [CrossRef]
181. Wiranarongkorn, K.; Patcharavorachot, Y.; Panpranot, J.; Assabumrungrat, S.; Arpornwichanop, A. Hydrogen and power generation via integrated bio-oil sorption-enhanced steam reforming and solid oxide fuel cell systems: Economic feasibility analysis. *Int. J. Hydrogen Energy* **2021**, *46*, 11482–11493. [CrossRef]
182. Gil, M.V.; Fermoso, J.; Pevida, C.; Chen, D.; Rubiera, F. Production of fuel-cell grade H_2 by sorption enhanced steam reforming of acetic acid as a model compound of biomass-derived bio-oil. *Appl. Catal. B Environ.* **2016**, *184*, 64–76. [CrossRef]
183. Fermoso, J.; Gil, M.V.; Rubiera, F.; Chen, D. Multifunctional Pd/Ni-Co catalyst for hydrogen production by chemical looping coupled with steam reforming of acetic acid. *ChemSusChem* **2014**, *7*, 3063–3077. [CrossRef] [PubMed]